Nansen Environmental and Remote Sensing Center

A non-profit
Research institute affiliated
With the University of
Bergen

NERSC

Thormøhlensgate 47
N-5006 Bergen,
Norway
http://www.nersc.no

NERSC Technical Report no. 291

SAR wind measurements over open ocean in the Svalbard area

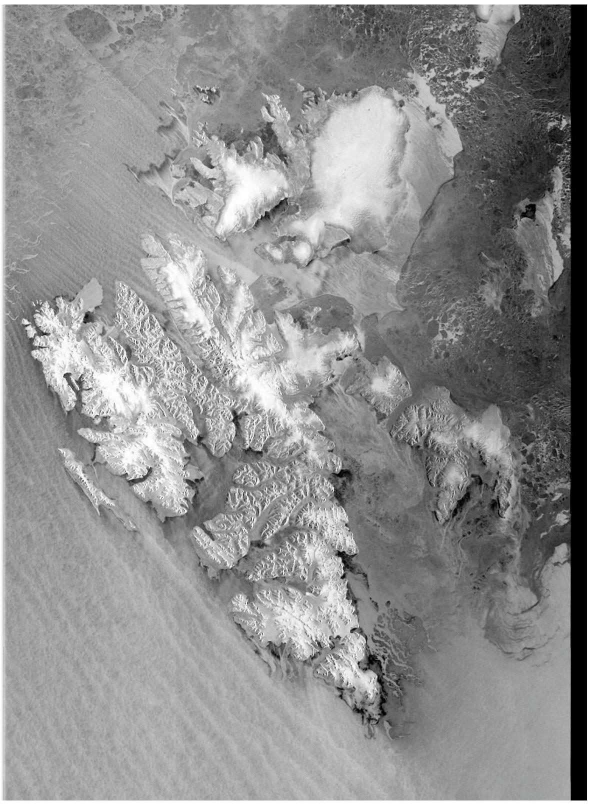

SAR image from ENVISAT obtained over Svalbard on 18 February 2008, showing northerly winds.

Project supported by Norwegian Space Centre

Contract JOP.07.06.2

February 2008

Authors:
Stein Sandven, Knut Frode Dagestad, Morten Hansen

	Nansen Environmental and Remote Sensing Center (NERSC) Thormøhlensgate 47 N-5006 Bergen, Norway Phone: + 47 55 20 58 00 Fax: + 47 55 20 58 01 E-Mail: Stein.Sandven@nersc.no http://www.nersc.no

TITLE: **SAR wind measurements over open ocean in the Svalbard area**	**REPORT IDENTIFICATION** **NERSC Technical report no. 291**
CLIENT Norwegian Space Centre	**CONTRACT** Contract no. JOP.07.06.2
CLIENT REFERENCE Terje Wahl	**AVAILABILITY** Customer report
INVESTIGATORS Stein Sandven, Knut Frode Dagestad Morten Hansen	**AUTHORISATION** Bergen, 18 February 2008 Stein Sandven

Contents

Executive Summary

The objective of this study has been to investigate the possibility to retrieve ocean surface wind from SAR images in the Svalbard area and the marginal ice zone. The CMOD4 wind algorithm has been implemented for use with ENVISAT ASAR Wideswath, Image Mode and Alternating Polarisation images. The algorithm runs automatically on ASAR images obtained from ESA rolling archive every day, using wind direction from NCEP fields. During the project a number of wind fields derived from SAR has been collected for different wind situations in the Svalbard area. The most important wind phenomena that have been observed in the SAR data are the gap winds (or jet streams) coming out of the valleys and straits. Also local wind structures outside the ice edge such as polar lows and wind fronts have also been observed. To validate the SAR-derived wind fields, we used data from an oceanographic buoy in the Barents Sea, localized southwest of Bjørnøya. This is one of two buoy that have been in operation since March 2007, providing data in realtime available from a website. It was first planned to use meteorological data from several met-stations around Svalbard, but the wind measurements for these buoys are biased by local topography. The wind data from the open ocean buoy southwest of Bjørnøya, taken near simultaneously with the SAR data, were extracted and compared with the SAR wind retrievals. In the period March – September we collected about 70 co-located data points which we used to make a quantitative comparison between the two data sets. The result of this comparison is that there is reasonable good agreement between the wind speed from SAR and from in situ measurements. The SAR wind speed is slightly higher than the in situ wind speed. Since the CMOD algorithm produces wind speed at 10 m height above the sea surface and the buoy provides wind data at 2 m height, some discrepancy between the two methods is expected. The SAR wind maps are disseminated via a webpage which is temporarily password-protected. The web site will be open after we have completed a validation period in 2008. The possibilities to provide operational wind fields from SAR has been investigated. The wind fields are produced automatically every time there is a SAR image available over open ocean provided from ESA rolling archive. At present there is limited SAR coverage over the study area, with typically 2 – 4 images per week. This is useful for research and demonstration work, but for fully operational monitoring it is necessary to obtain SAR wind fields twice per day in the Svalbard area and the marginal ice zone. The SAR wind data are presently tested by met.no in the ArcChange and OOMM projects. Further studies of SAR wind is conducted in the ongoing ESA project "SAR ocean wind, waves and currents".

1. Introduction and background

Studies of SAR wind retrieval in the Svalbard region started in 1995 when a field experiment was conducted with RV Håkon Mosby, as shown in Fig. 1 (Furevik et al., 2002). During the experiment in situ measurements of oceanographic and atmospheric measurements were obtained form the ship, satellite SAR data were obtained from ERS-1 and mesoscale atmospheric modelling was done after the experiment. The wind situation shown in Fig. 1 was easterly 4 -6 m/s north of Svalbard, with a strong jet stream of 12 – 14 m/s blowing though the Hinlopen Strait from southeast. The SAR derived wind field using the CMOD algorithm, as well as the MM5 mesoscale atmospheric model could identify this jet stream. The ship track of Håkon Mosby was located perpendicular to this jet and in situ data could therefore document the wind speed and direction of the jet stream.

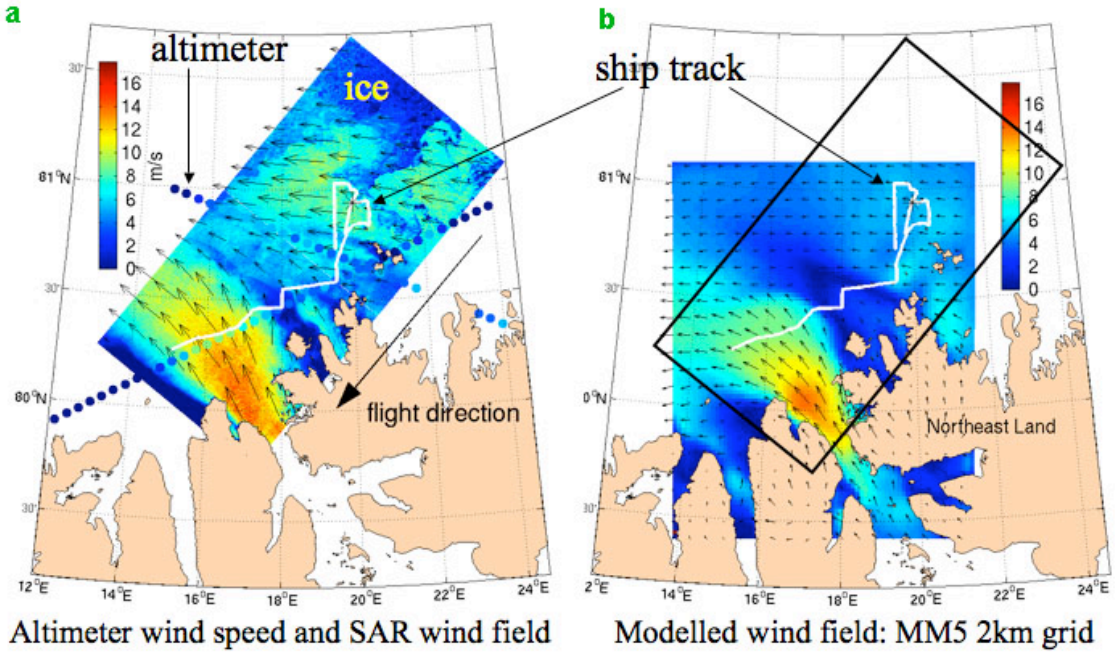

Figure 1. (a) SAR-derived wind speed and direction north of Svalbard in August 2005, with radar altimeter tracks and ships track superimposed; (b) simulation of the wind field at the same time as the SAR images was obtained, using the MM5 mesoscale meteorological model at the Geophysical Institute, University of Bergen (Furevik et al., 2002).

The large-scale wind fields from scatterometers, which is the major data source for ocean winds, do not resolve the detailed wind structure around the Svalbard archipelago. Wind scatterometer on satellites such as Quikscat delivers wind fields with 25 km resolution, and these data are the main source for operational wind measurments over the ocean for the weather forecasting models (Fig. 2). The most commonly used atmospheric forcing fields have typical 25 km resolution (NCEP, ECMWF).

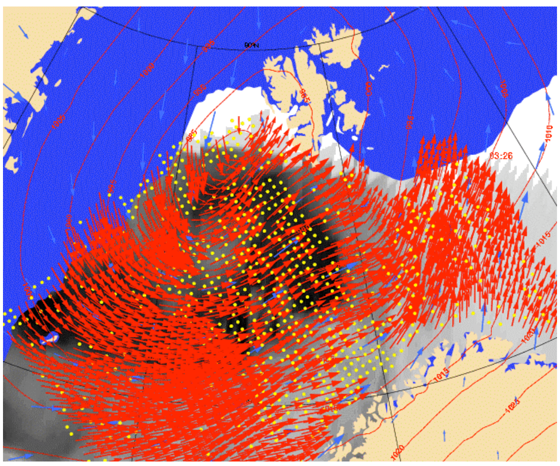

Figure 2. Example of Quickscat 25 km resolution wind field in the Norwegian Sea (16 February 2008). The blue area is sea ice mask. (Source: Eumetsat SAF product, http://www.knmi.nl/scatterometer/).

2. SAR coverage in the Svalbard and Barents Sea area

The 35-day repeat cycle of ENVISAT has a subcycle of three days which provides nearly repeated coverage every three days. At high latitudes, above 70 N, Wideswath images can in theory give complete coverage every day. But in practice, the coverage by Wideswath images is more scattered, as shown in Fig. 3. There are plenty of SAR images available in the Svalbard area for research and development work as well as for demonstration of operational monitoring systems. For the SAR wind retrieval around Svalbard, there have been typically 1 – 2 wideswath scenes per week during 2007. Wind retrieval is done automatically for all SAR images (obtained in open water areas). In order to use satellite data for operational wind monitoring, it is necessary to obtain new data several times per day, such as is done by wind scatterometers from Quikscat and ASCAT.

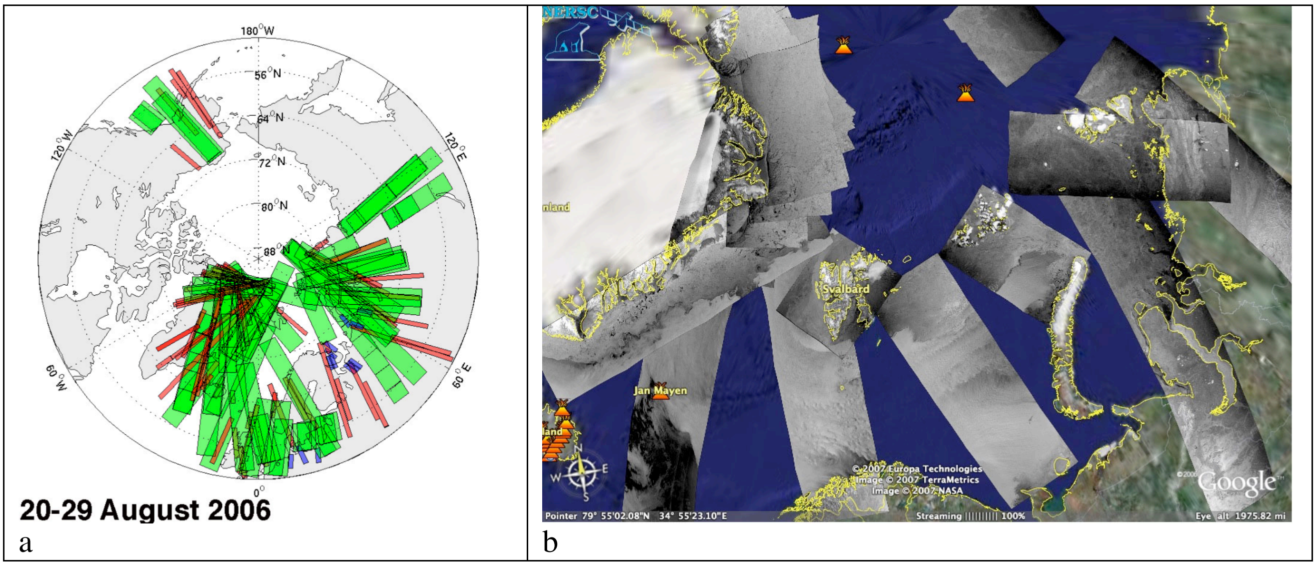

Figure 3. Example of ENVISAT ASAR coverage in the Barents Sea area, provided by ESA rolling archive. (a) Composite of stripes of Wideswath (green), Image Mode (red) and Alternating Polarization (blue) collected during 10 days in August 2006; (b) Wideswath coverage in the Svalbard region 18 – 22 February 2007.

3. The SAR wind algorithm

The CMOD-4 model function is an empirical function that relates the normalised radar cross section (sigma0) to near surface wind speed, wind direction relative to radar look direction, and radar incidence angle. The principle is that sigma0 is a measure of the ocean surface roughness on the order of the wavelength of the sensor (C-band, ~5 cm), which is again correlated with the wind speed. The function was tuned to sigma0 measurements from the ERS-1 scatterometer and 10 m winds from the ECMWF model. Although it was tuned to scatterometer data, it has proven to be valid for SAR sensors also operating at C-band, such as e.g. Envisat ASAR. The radar incidence angle is well known, and if the wind direction is also known, the wind speed can be inverted from measured sigma-0 using the CMOD-4 model function. The wind direction can be taken either from a numerical forecast model, from scatterometers, or from in situ measurements (such as a buoy). In some cases when signatures of wind aligned boundary layer rolls are visible on the SAR image, the wind direction can be inferred directly from the image with FFT methods. In this study we have used wind directions both from the NCEP global forecast system and from the buoys to retrieve the wind speed from ENVISAT ASAR images.

4. Characteristic wind patterns observed in the SAR data

The topography of the Svalbard archipelago generates many local wind patterns that can be observed in the SAR wind maps generated during 2007. Also in the marginal ice zone several specific wind patterns can be found. Figs. 4 and 5 show selected examples of SAR images in greyscale and corresponding wind speed in colours and direction by arrows. In Fig. 4a easterly winds blows off the ice edge south of Westspitzbergen, showing characteristic stripes along the wind direction. There is also a small low with a wind front and a local wind maximum to the west of Isfjorden. Fig. 4b shows south-easterly winds in August when the ice edge is located north of Svalbard. There is a jet with maximum wind speed north of Hinlopen strait, caused by intensification of the easterly wind passing through the strait.

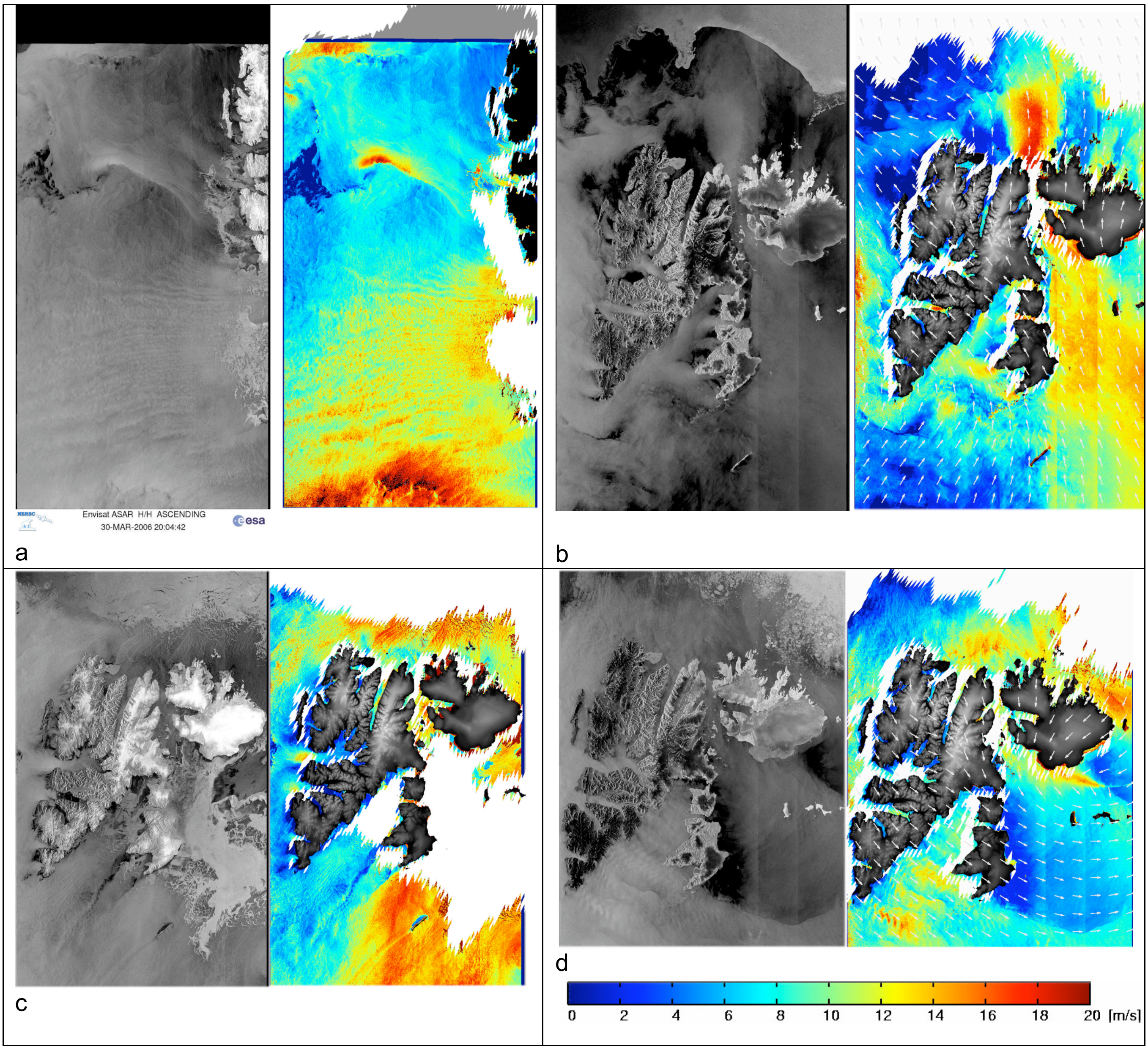

Figure 4. Examples of SAR wind fields around Svalbard: (a) 30 March 2006, (b) 07 August 2007, (c) 10 January 2008; (d) 20 August 2007. Note that wind direction is not shown in (a) and (c).

Fig. 4 c shows example of northerly winds in January when there is ice east of Edgeøya. North of Svalbard has open water showing maximum wind speed off the ice edge. There is also intensification of the wind speed off the ice edge in the Hopen area. Fig 4 d shows an example of westerly winds in the southern part of Svalbard, and northerly winds in the northern part in August. Some intensification of the wind field is outside the ice edge north of Nordaustlandet.

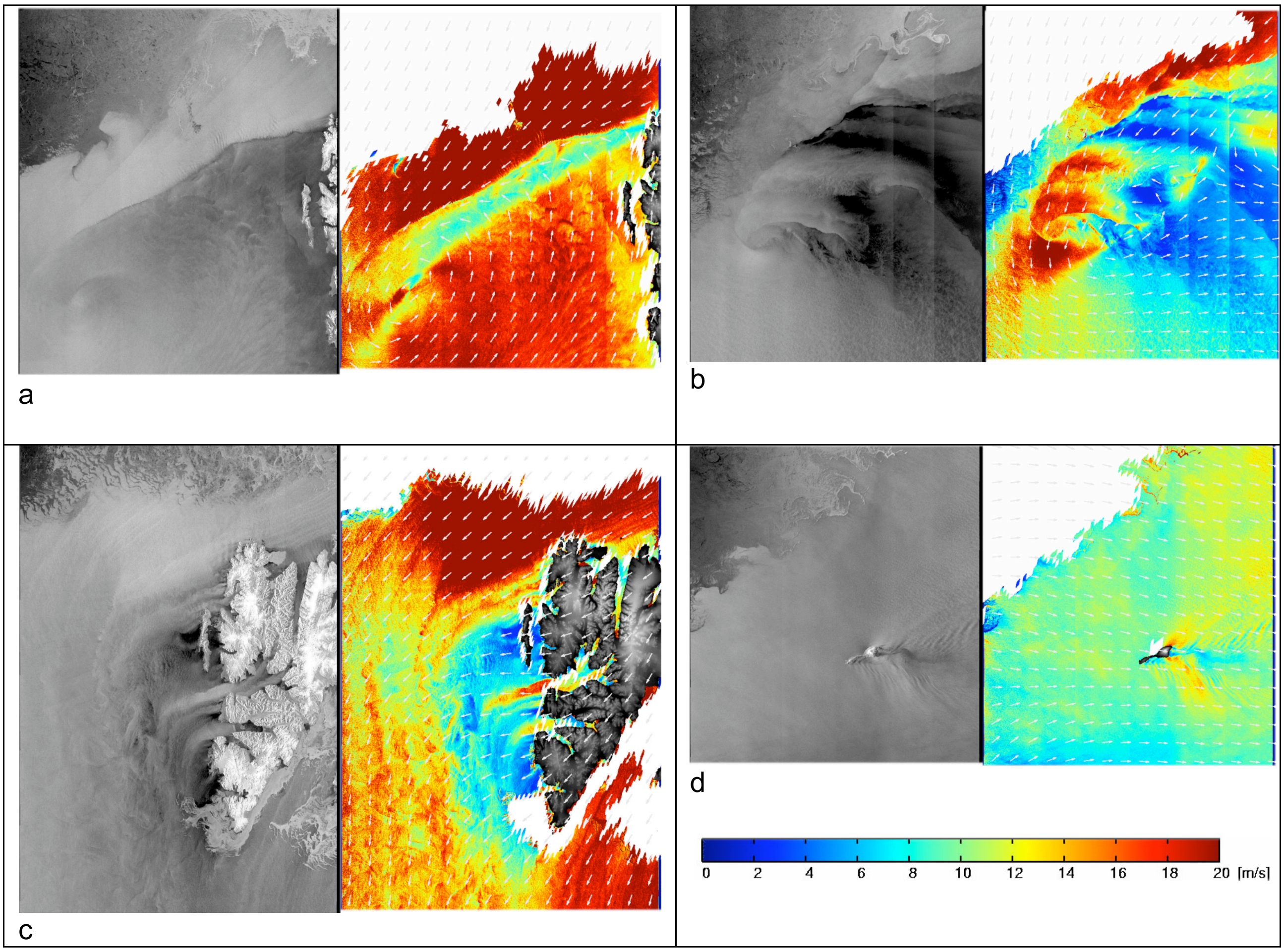

Figure 5. Examples of SAR wind patterns around Svalbard: (a) 23 December 2007, (b) 25 January 2008, (c) 31 January 2008; (d) 13 February 2008.

In Fig. 5a there is a very pronounced wind front along the ice edge west of Svalbard. The wind speed is stronger near the ice edge and weaker to the south of the front. The wind speed calculation in the frontal zone is not very accurate because the NCEP wind direction changes by 180°. A polar low is shown in Fig 5b, with a strong wind front along the ice edge north of the polar low. An example of strong northeasterly wind is shown in Fig. 5c, where the west coast of Svalbard is sheltered as indicated by the lower wind speed, but with two jet streams coming out of Isfjorden and VanMijenfjorden. In Fig 5d westerly winds are blowing over Jan Mayen, generating atmospheric wave patterns on the lee side. There are many other examples of topographic effects on the wind fields observed in SAR images caused by the 2277 m high Beerenberg mountain on Jan Mayen. More examples of SAR wind structures are presented in Annex A.

5. Validation by data from an oceanographic buoy

The most suitable in situ data sets for validation of the SAR wind retrievals are buoy data from two oceanographical buoys deployed in the Barents Sea in March 2007. The buoys are located at 73.5 N 15.5 E (southwest of Bjørnøya) and at 74.0 N 30.0 E (east of Bjørnøya) as shown in Fig. 6 a. Standrard meteorological and sea surface data are collected every 10 minutes and transmitted by satellite to land, where data can be accessed from http://www.oceanor.com/Barents_Sea/. The buoys are funded by Statoil and operated by Oceanor. Example of real-time data are shown in Fig. 6 b, where windgust is shown in blue and 10 minutes mean wind speed in red.

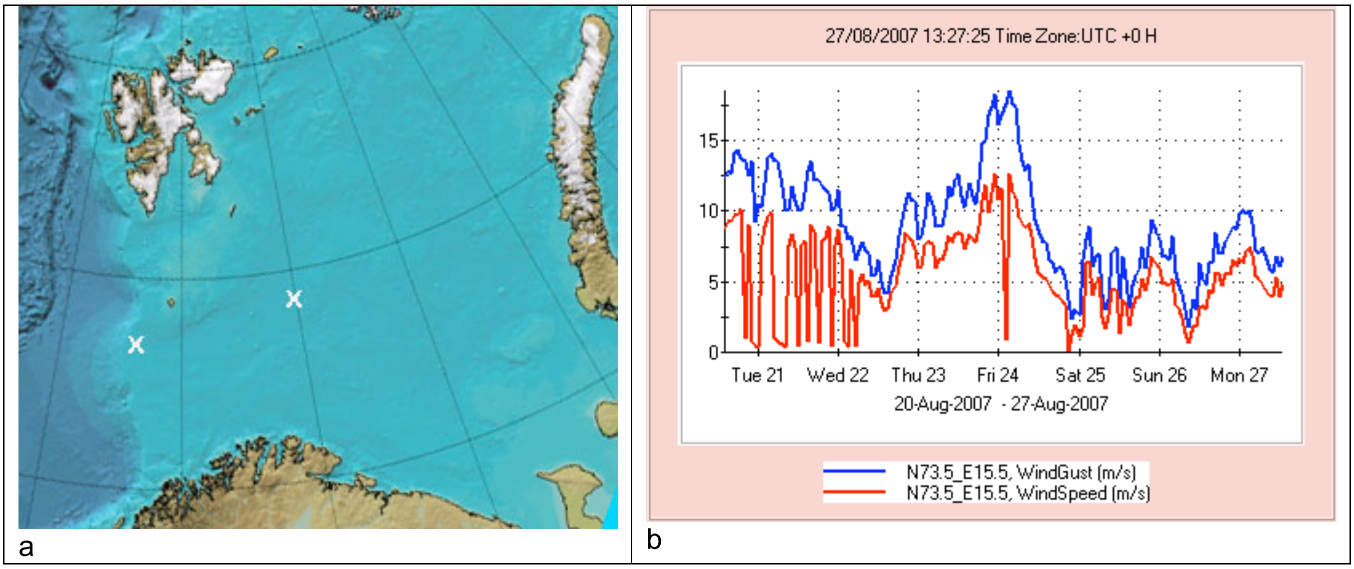

Figure 6. (a) Map of the Barents Sea with localisation of the two met-ocean buoys that have produced real time data since March 2007; (b) example of wind measurements from the western buoy during one week in August 2007.

Wind speed and direction obtained from SAR data in the grid cell coinciding with the westernmost buoy position are compared with buoy data for the validation period from March to September 2007. About 70 co-located data points of SAR wind measurements were collected in this period. Data from the easternmost buoy were not used, because much fewer SAR data were collected in this area compared to the westernmost buoy. Time series of wind speed and direction from SAR data and buoy data are presented in Fig. 7 a-g, with data for one month in each plot.

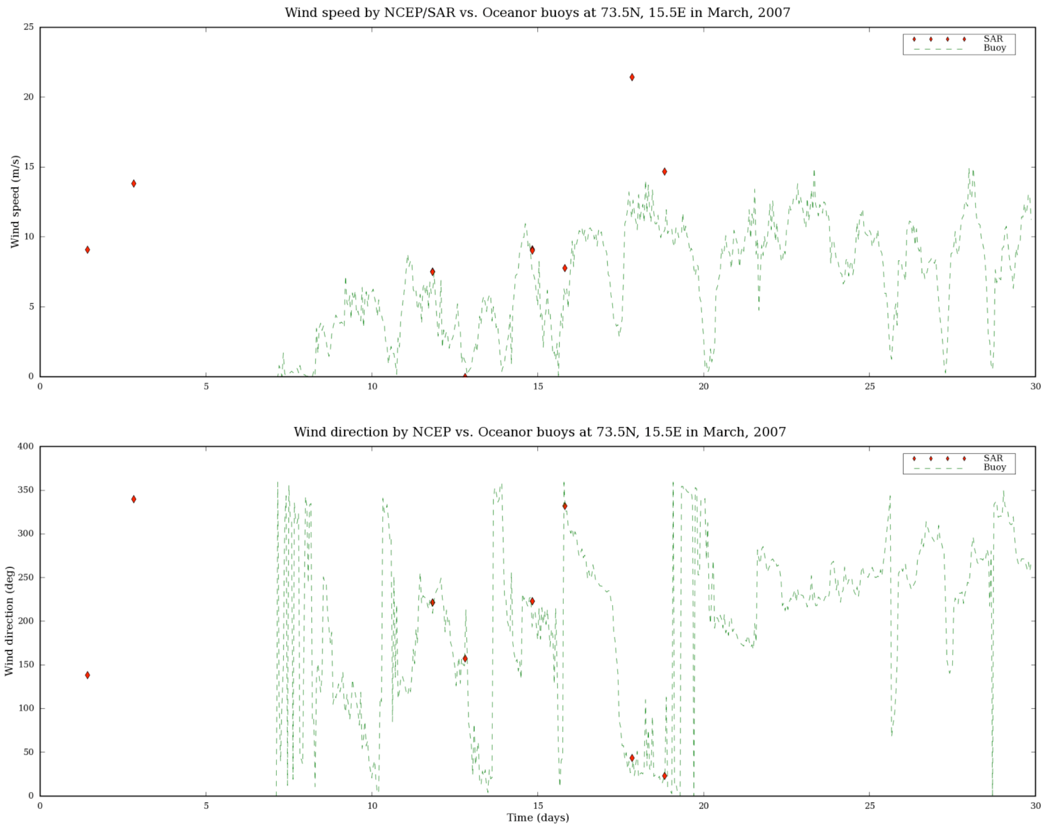
Wind speed by NCEP/SAR vs. Oceanor buoys at 73.5N, 15.5E in March, 2007
Wind speed (m/s)
SAR
Buoy
Wind direction by NCEP vs. Oceanor buoys at 73.5N, 15.5E in March, 2007
Wind direction (deg)
Time (days)

a)

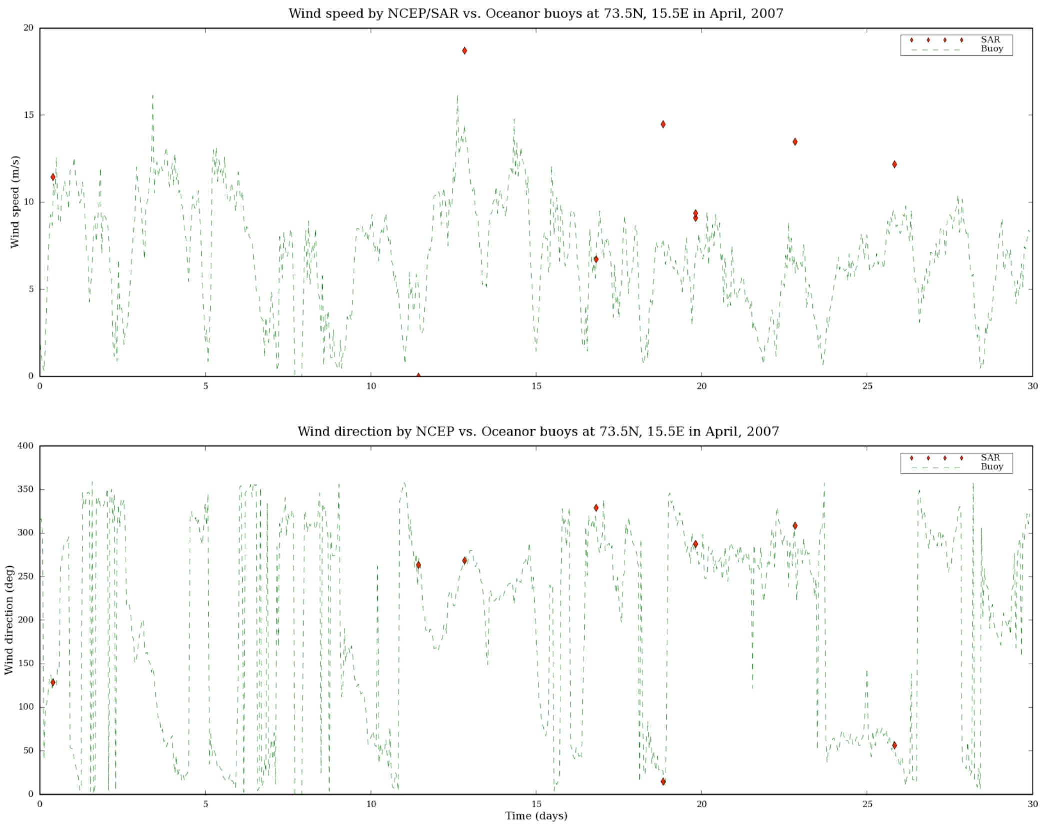
Wind speed by NCEP/SAR vs. Oceanor buoys at 73.5N, 15.5E in April, 2007
Wind speed (m/s)
SAR
Buoy
Wind direction by NCEP vs. Oceanor buoys at 73.5N, 15.5E in April, 2007
Wind direction (deg)
Time (days)

b)

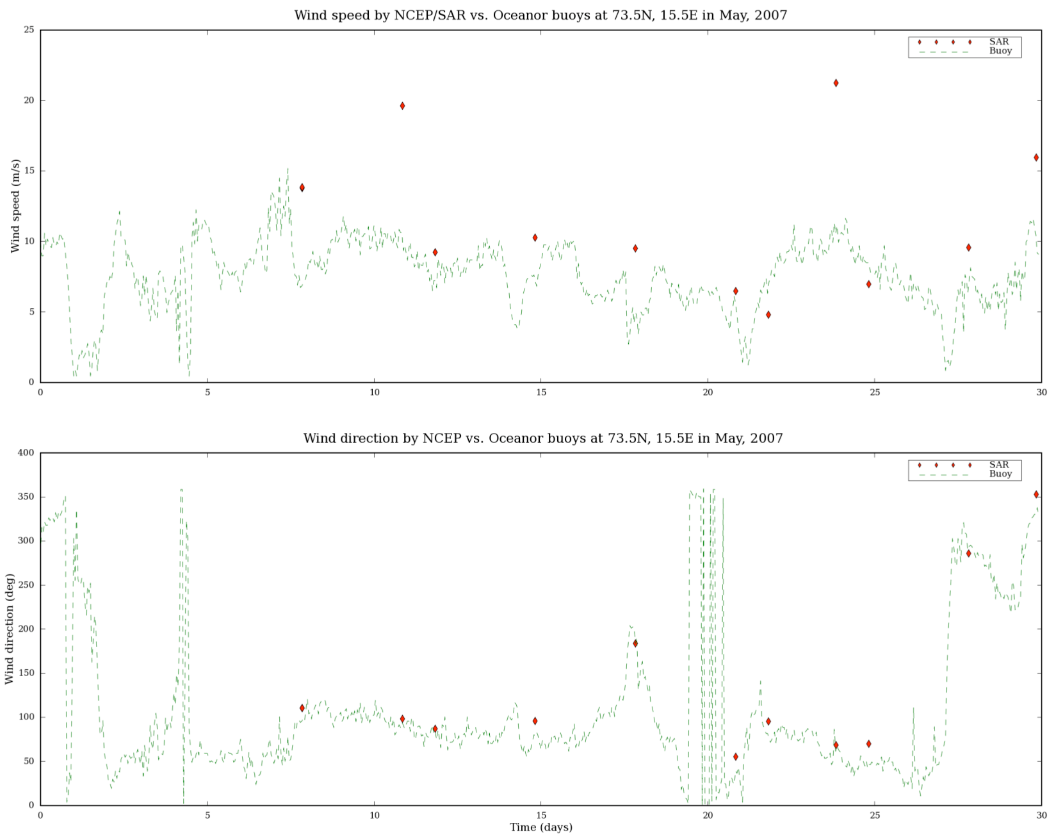
Wind speed by NCEP/SAR vs. Oceanor buoys at 73.5N, 15.5E in May, 2007
Wind speed (m/s)
SAR
Buoy
Wind direction by NCEP vs. Oceanor buoys at 73.5N, 15.5E in May, 2007
Wind direction (deg)
SAR
Buoy
Time (days)

c)

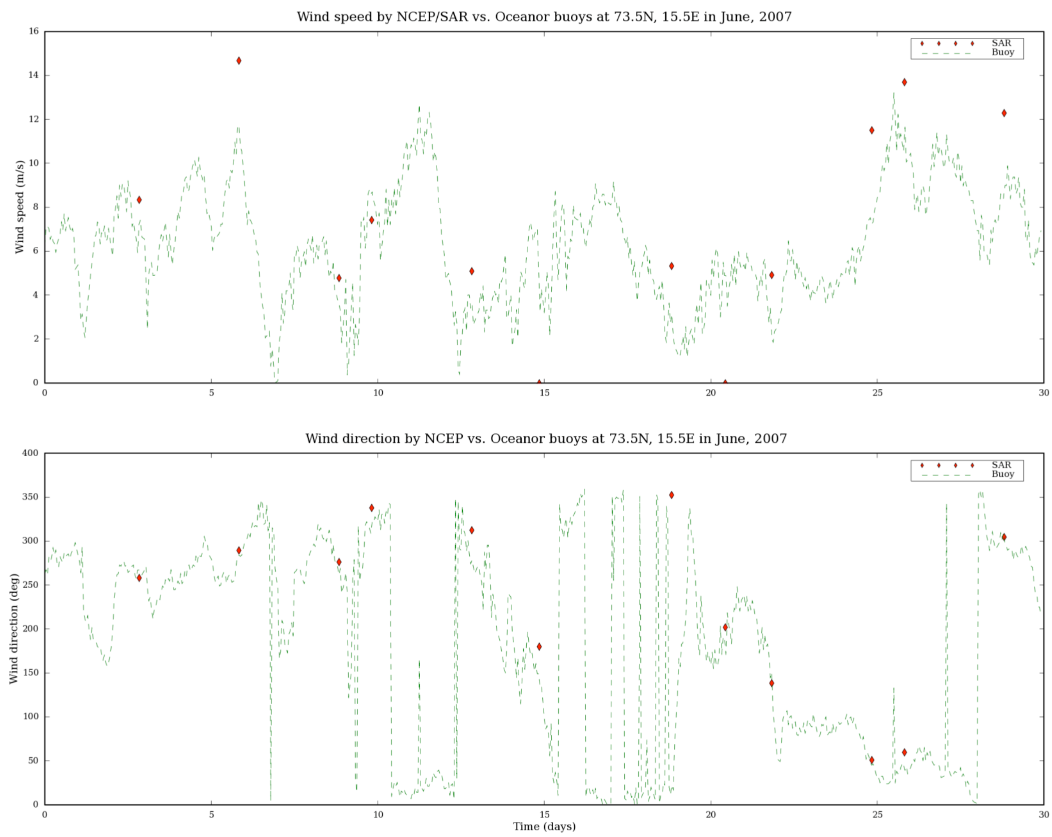
Wind speed by NCEP/SAR vs. Oceanor buoys at 73.5N, 15.5E in June, 2007
Wind speed (m/s)
SAR
Buoy
Wind direction by NCEP vs. Oceanor buoys at 73.5N, 15.5E in June, 2007
Wind direction (deg)
SAR
Buoy
Time (days)

d)

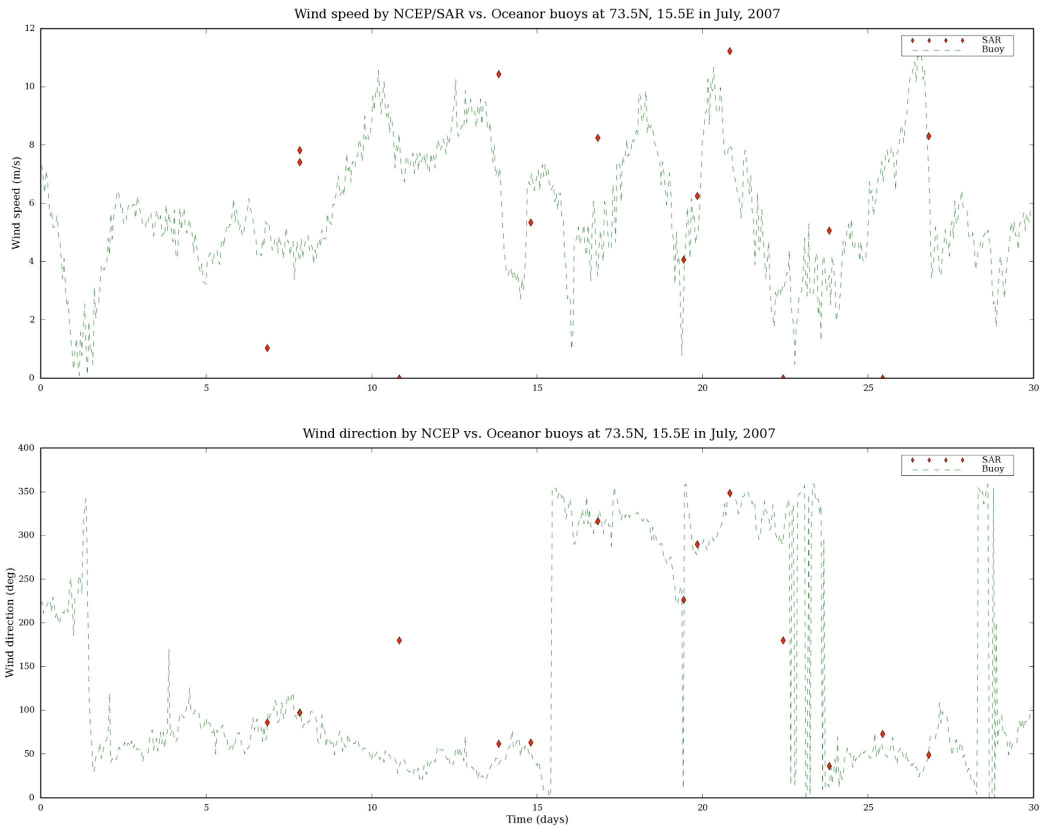
Wind speed by NCEP/SAR vs. Oceanor buoys at 73.5N, 15.5E in July, 2007
SAR
Buoy
Wind speed (m/s)
Wind direction by NCEP vs. Oceanor buoys at 73.5N, 15.5E in July, 2007
SAR
Buoy
Wind direction (deg)
Time (days)

e)

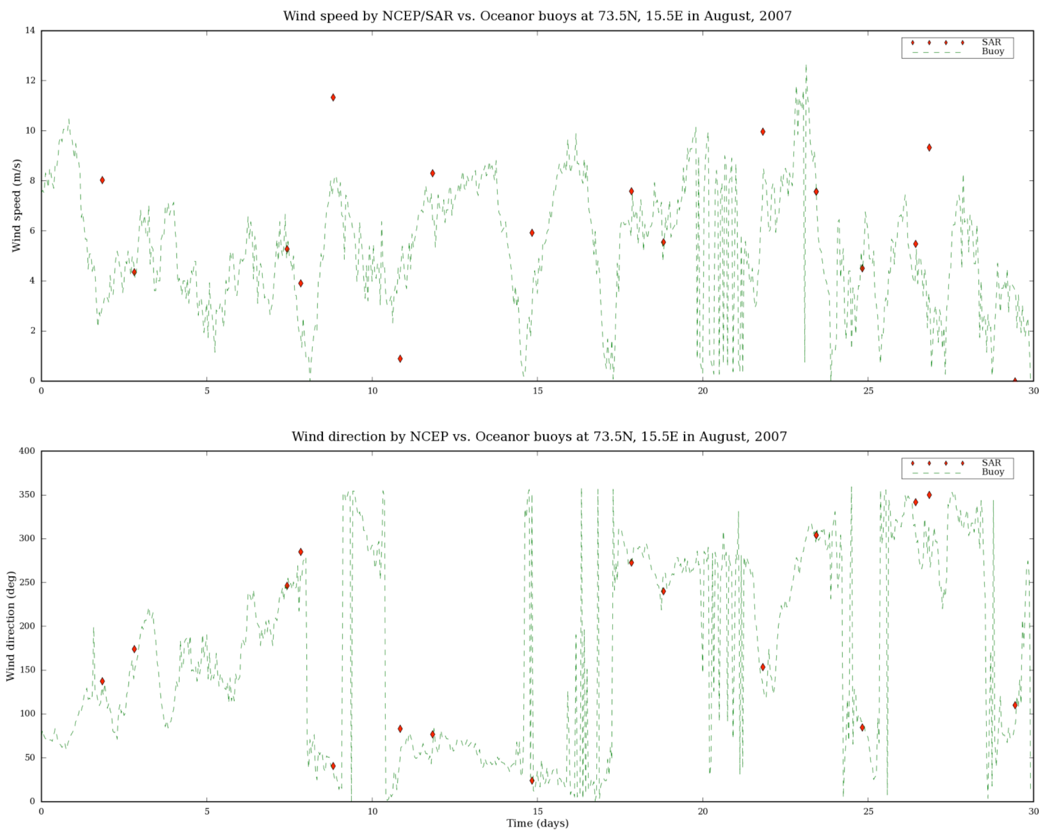
Wind speed by NCEP/SAR vs. Oceanor buoys at 73.5N, 15.5E in August, 2007
SAR
Buoy
Wind speed (m/s)
Wind direction by NCEP vs. Oceanor buoys at 73.5N, 15.5E in August, 2007
SAR
Buoy
Wind direction (deg)
Time (days)

f)

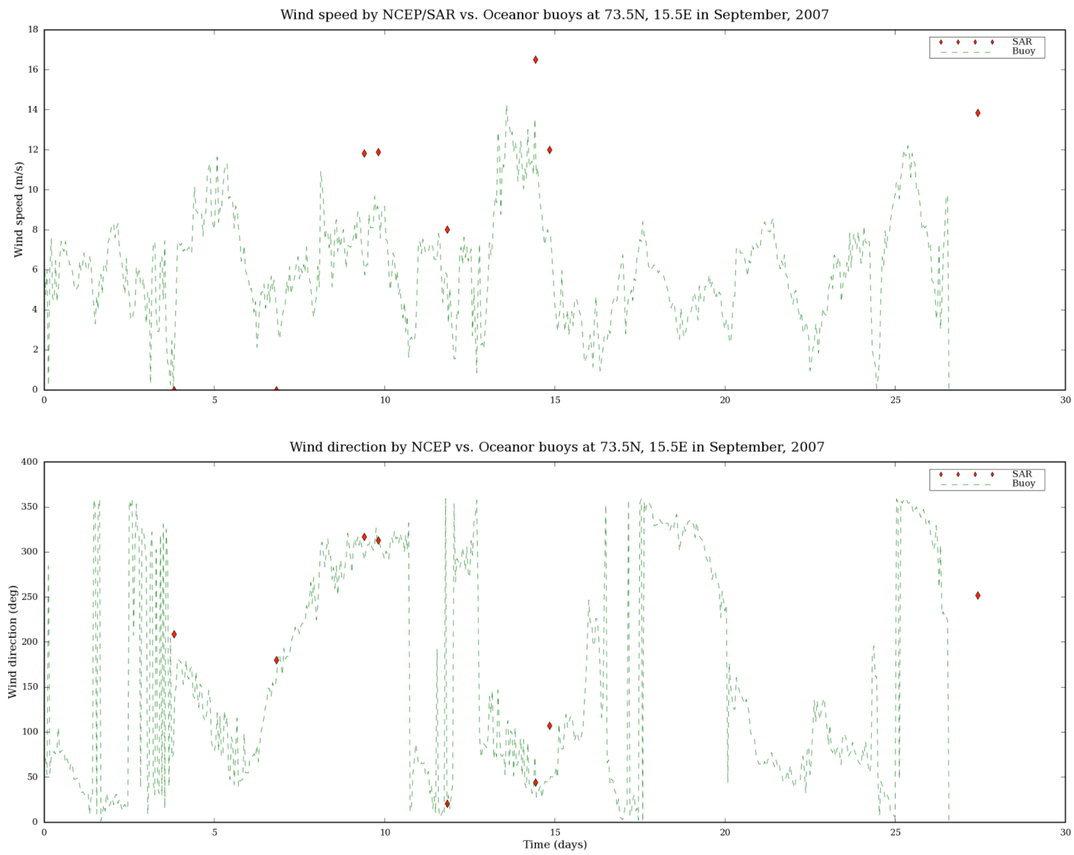

g)

Figure 7 (a-g). Monthly time series of wind speed (upper graph) and wind direction (lower graph) from hourly buoy data are shown by the dashed curves, while wind speed from SAR and direction from NCEP are shown by red dots.

The wind speed and direction from the buoys obtained within +- 30 minutes of the SAR data are plotted together with the SAR-derived wind data for the period from March to September, as shown in Fig. 8. SAR wind speeds below 4 m/s are not included because the CMOD algorithm is not valid below this threshold. Buoy wind speeds below 2 m/s are also excluded to avoid any comparisons at very low wind speeds. The most interesting result is that the SAR wind speed is generally higher than the buoy wind, especially in the winter-spring months. For the summer months the difference is smaller (Fig. 8a). Apart from this bias, which must take into account that SAR wind is instantaneous and buoy wind is 10 minute average, there is good agreement between the wind speed from the two data sets. The average difference between the two methods is about 3 m/s and the standard deviation is 2.6 m/s for the data set presented in Fig. 8.

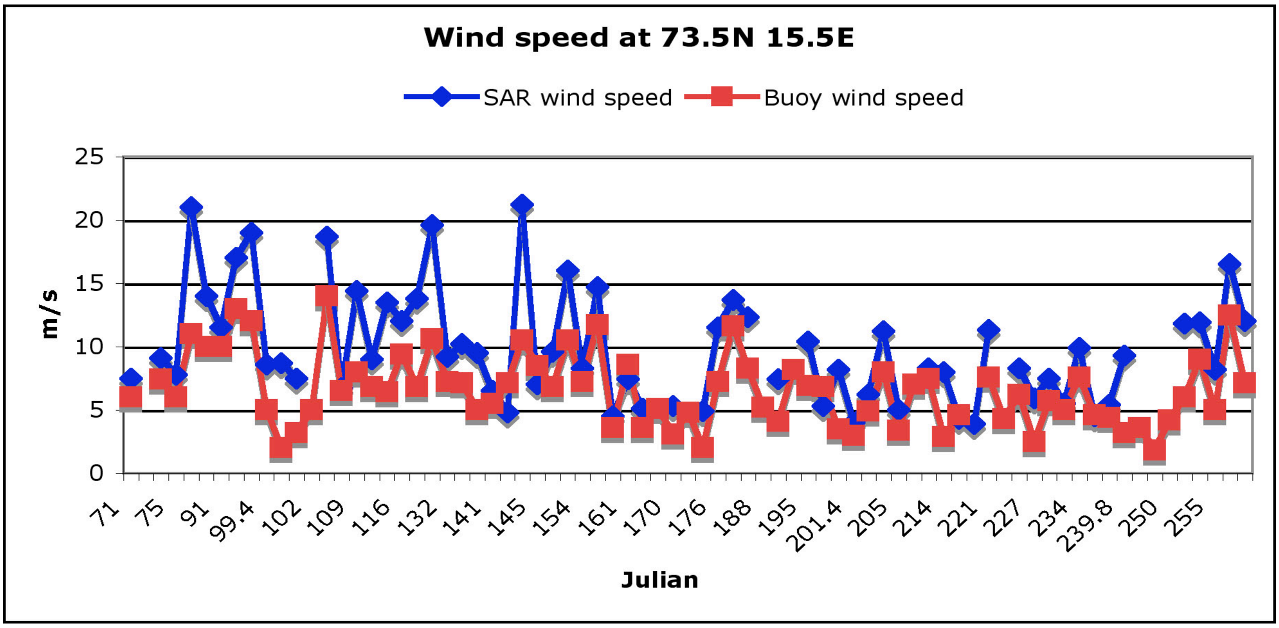

a

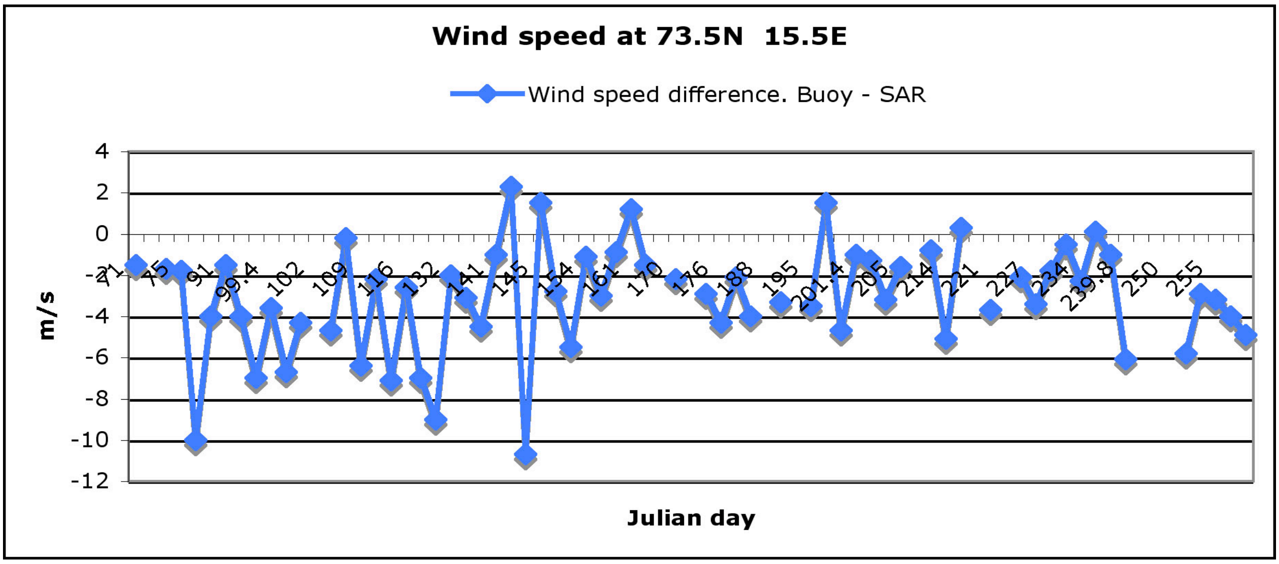

b

Figure 8. (a) Wind speed from SAR (blue graph) and wind speed from buoy data (red graph) for about 70 co-located data points; (b) wind speed difference between the two data sets.

For wind direction, the comparison is between NCEP direction and buoy direction, as shown in Fig. 9 a. The wind direction is not retrieved for the SAR image in this study, but there are methods to extract wind direction from the SAR image directly. The comparison shows very good agreement between the two data sets, except for a few data points (Fig. 9 b). This shows that NCEP gives quite good wind direction data in the open ocean area where the buoys are located.

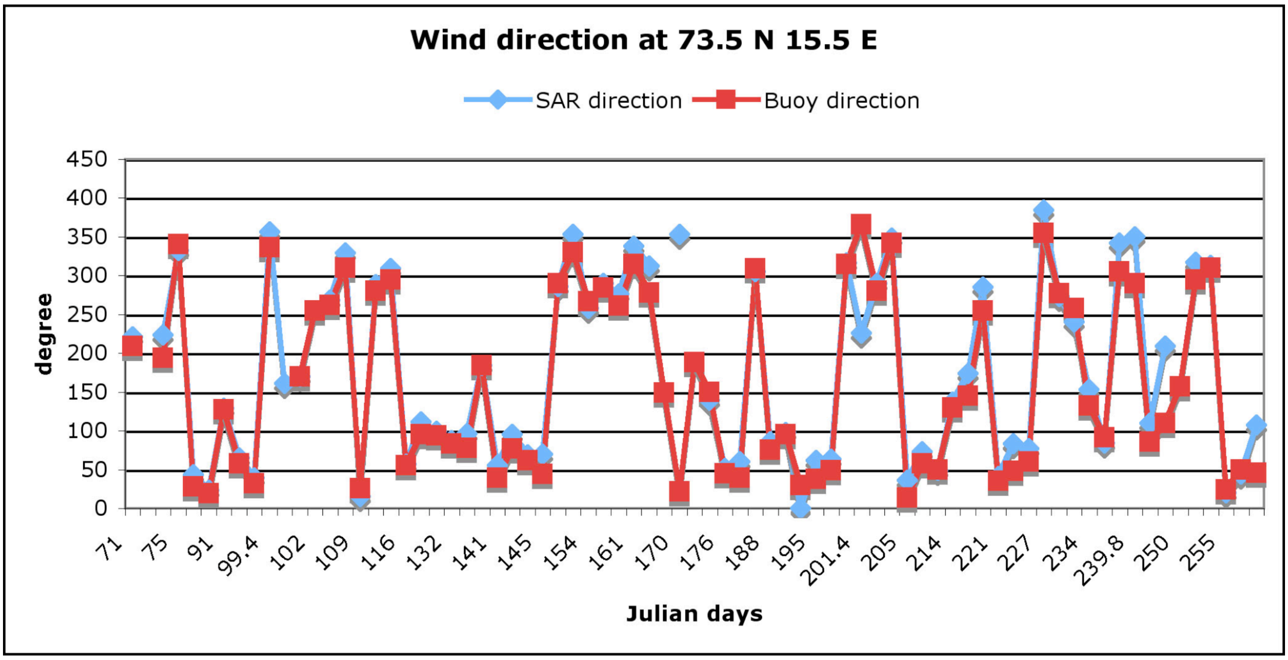

a)

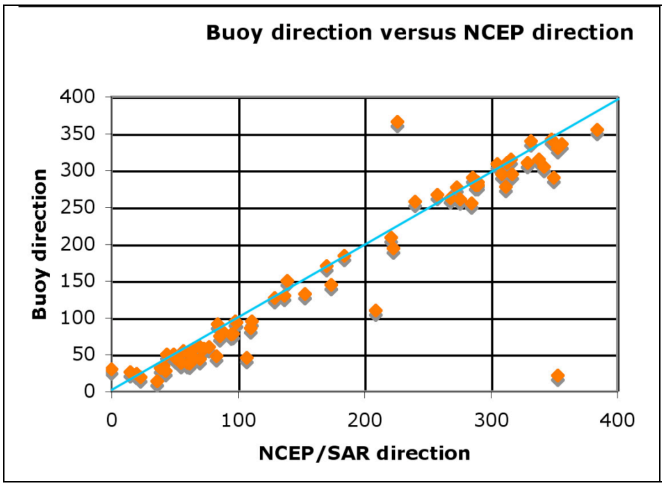

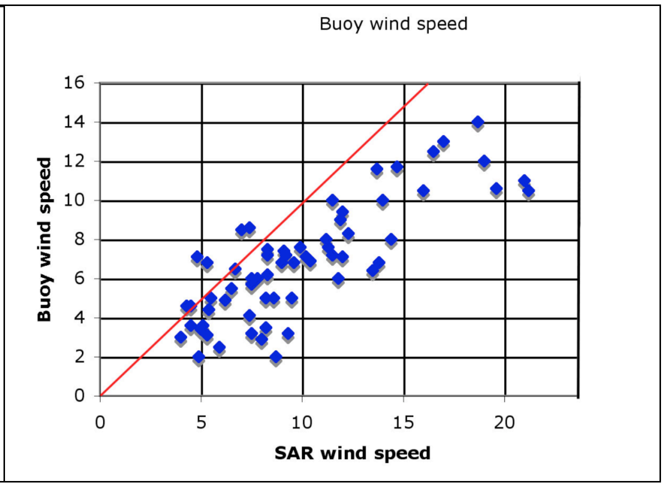

b) c)

Figure 9. (a) Wind direction NCEP (blue graph) and buoy (red graph) for the 70 co-located SAR and buoy data; (b) scatter plot of buoy direction versus NCEP direction; (c) scatter plot of buoy wind speed versus SAR wind speed

6. Conclusions and further work

SAR wind retrieval with the CMOD4 algorithm have been used to produce high-resolution wind fields over open sea in the Svalbard area and the marginal ice zone north and west of Svalbard. The first studies of SAR wind in the Svalbard region was done by Furevik et al. (2002), while coastal wind retrieval from SAR in southern Norway has been demonstrated by Korsbakken et al., (1998). More extensive mapping of coastal winds from SAR data has been done by Beal et al., (2005) who have produced an atlas of RADARSAT SAR wind fields from south coast of Alaska. These studies have shown that SAR can provide high—resolution wind fields showing local wind patterns caused by land topography, atmospheric fronts and other phenomena in the marginal ice zone. In this project, wind field maps have been produced where wind direction is taken from NCEP fields and wind speed from ENVISAT ASAR Wideswath images. An automated procedure has been established for downloading and processing SAR images obtained from ESA rolling archive every day. During the project a number of wind fields derived from SAR has been collected for different wind situations in the Svalbard area. The most important wind phenomena that have been observed in the SAR data are the gap winds (jet streams) coming out of the valleys and straits. Also local wind structures outside the ice edge such as lows and wind fronts have also been observed. The SAR wind retrievals have been validated by wind data from a buoy in the Barents Sea. About 70 co-located measurements of wind fields from the buoy and from SAR/NCEP data were obtained in the period from March to September 2007. These data have been compared quantitatively, showing reasonably good agreement. The wind speed from SAR is generally higher than wind speed from the buoy. This is explained by the fact that the CMOD algorithm calculates wind speed at 10 m height above sea surface, while wind measurements from the buoy were obtained at 2 m height. This validation was done in open sea without any influence from land topography or sea ice. It is also planned to carry out validation in a fjord, based on meteorological data from an automated weather station in Storfjorden. If these data are successfully obtained, further validation of the SAR wind retrieval will be done in 2008. There are several methods for retrieval of wind direction directly from the SAR image, for example to use Fast Fourier Transformation to determine the direction of the characteristic wind stripes that are often visible in SAR images of open ocean. There are ongoing efforts to improve the CMOD algorithm to provide more accurate estimates of wind speed in areas of low fetch. Mesoscale meteorological models, such as MM5, can produce similar wind fields as observed in SAR, as shown by Furevik et al., (2002). In the ongoing ESA project “SAR ocean wind, waves and currents” we are investigating how SAR-generated mean wind fields can be used to add details to the operational weather forecasts. This approach avoids the problem of large time interval between successive SAR images covering the same area. Further work should include more systematic comparison of local wind patterns from SAR and MM5 simulations. This will be a useful activity to learn more about the processes determining local wind phenomena in fjords and in the marginal ice zone. Further work should also include production of a wind climatology in Svalbard area based on SAR data. This work should be based on SAR data acquired over several years. Finally, the effect of varying atmospheric stability on SAR wind retrieval should be studied. This can be done by using atmospheric profile data from radiosondes and stability estimates form models. The usefulness of SAR wind retrievals will increase when Sentinel-1 data become available, allowing more frequent data acquisition. In operational weather and sea ice forecasting, it is necessary to have wind measurements several times per day. It is expected that satellite SAR data can play an increasingly important role to provide high-resolution wind fields in coastal and sea ice areas.

7. References

Furevik, B.R., O.M. Johannessen, A.D. Sandvik: *SAR - retreived wind in Polar Regions-comparison with in situ data and atmospheric model output.* In IEEE Transaction on Geoscience and Remote Sensing. Vol. 40, nr. 8, 2002.

Beal R., Young G., Monaldo F. et al. High resolution wind monitoring with wide swath SAR: A user's guide, NOAA/NESDIS/ORA, Washington DC, 2005. 155 pp.

Korsbakken E., Johannessen J.A., Johannessen O.M. Coastal wind field retrievals from ERS synthetic aperture radar images. J. Geophys. Res. 1998. V. 103. № C4. P. 7857–7874.

Annex 1. Plot of SAR wind maps over the validation site

Period: March – September 2007

Date and time in GMT is shown for each map

The validation site located at 73.5 N 15.5 E is marked by a white circle in each map

White areas indicate ice mask provided from passive microwave data

Wind direction is indicated by the white arrows

Wind speed is indicated by the following colour bar:

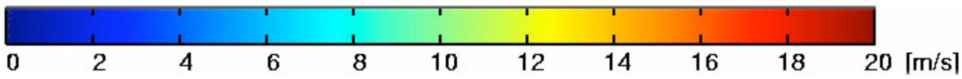

02 March 10:17

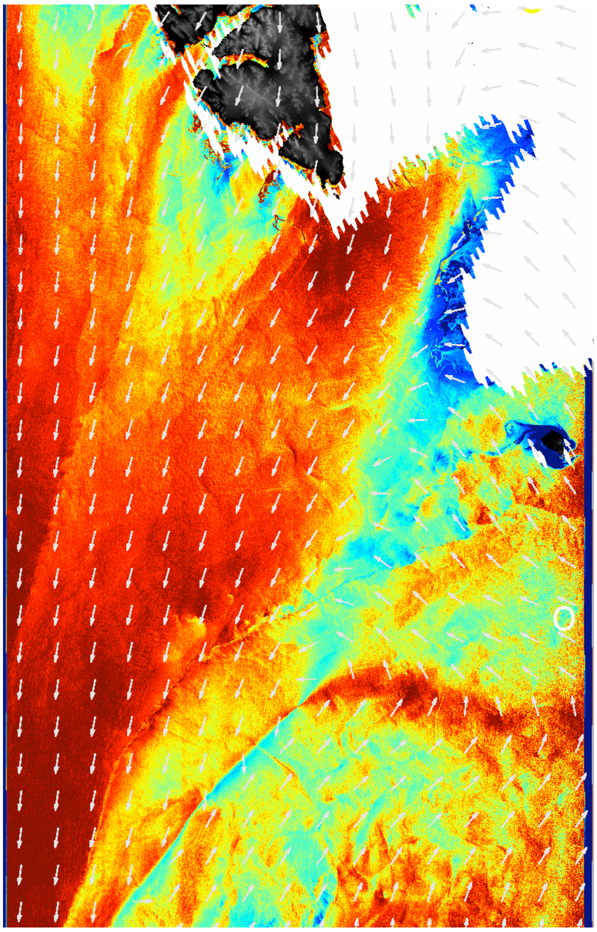

12 March 19:57

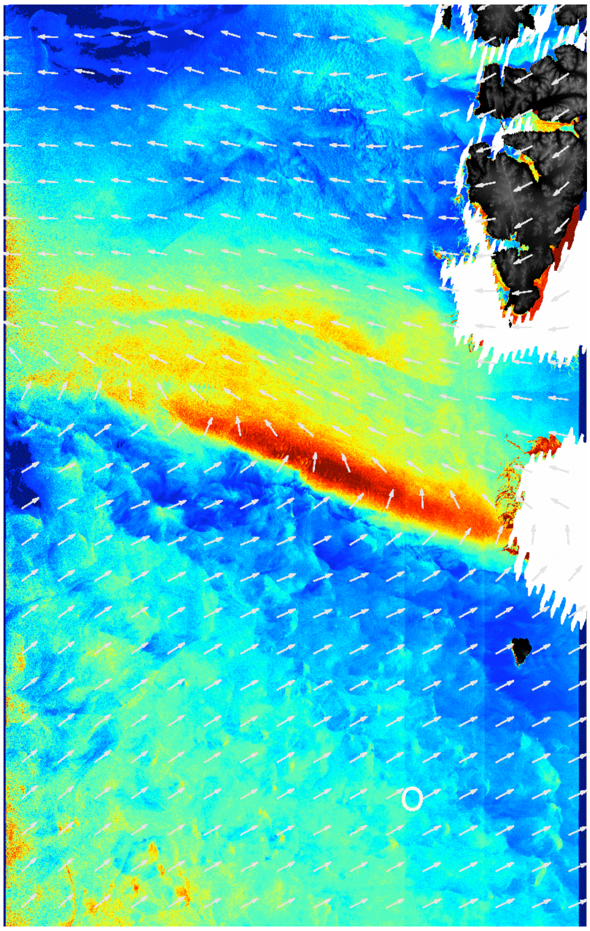

03 March 19:41

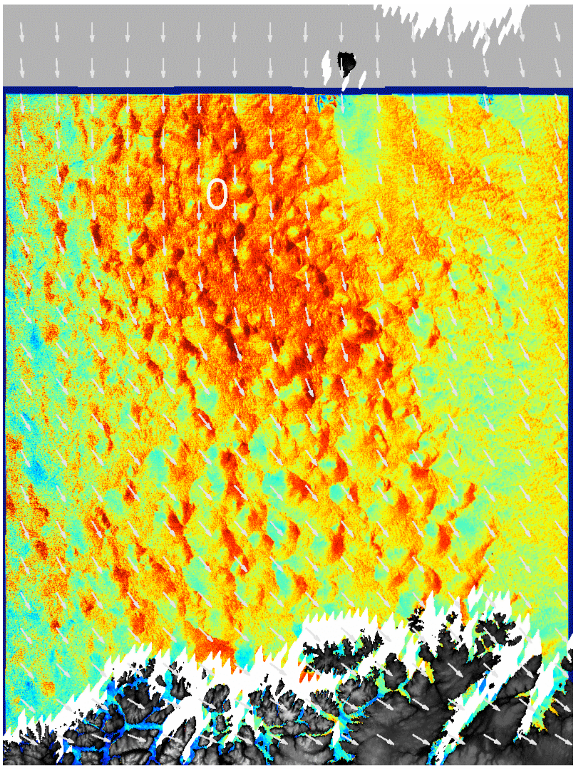

13 March 19:26

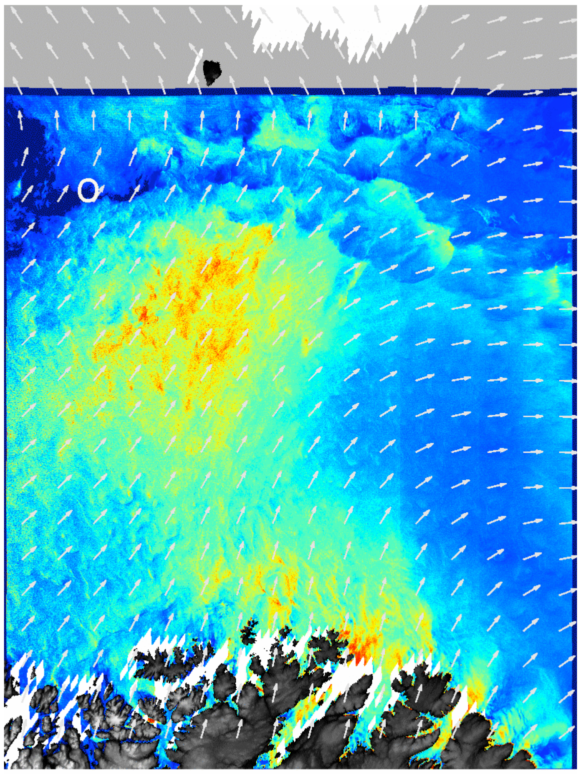

15 March 20:02

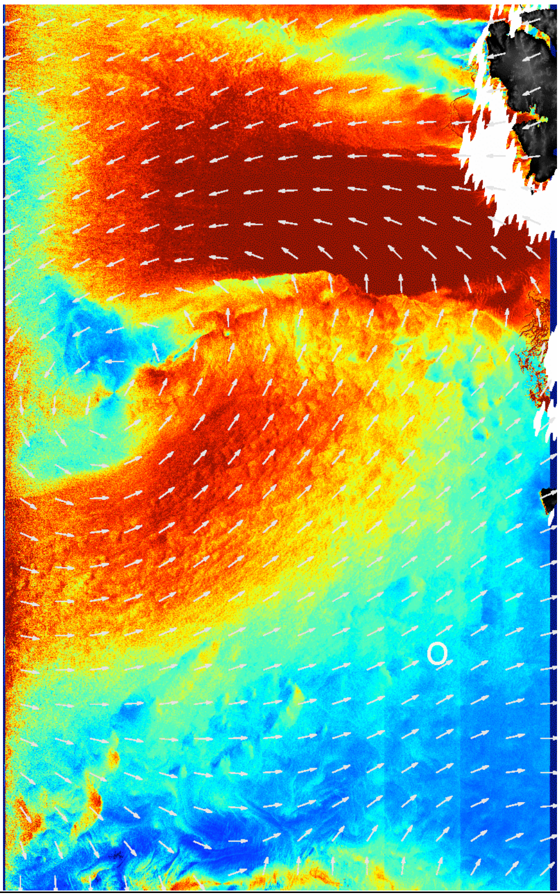

18 March 20:06

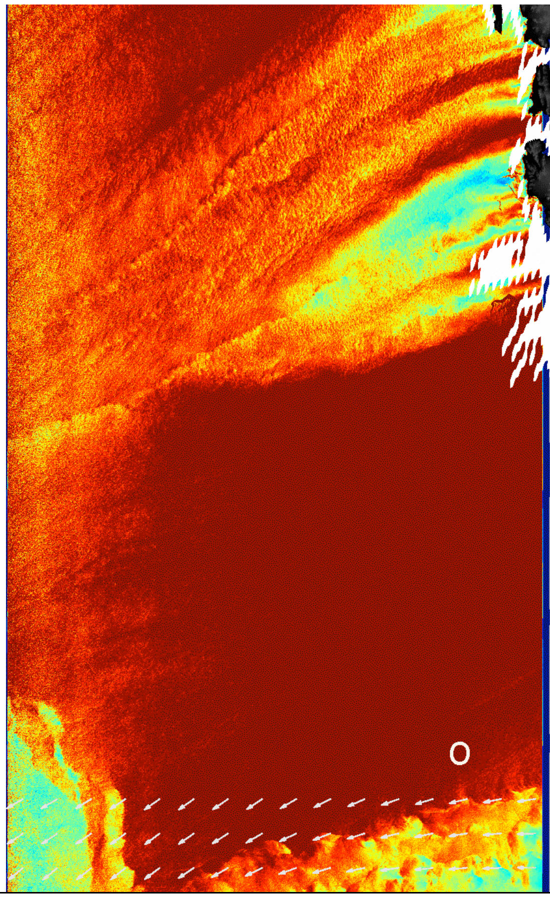

16 March 19:32

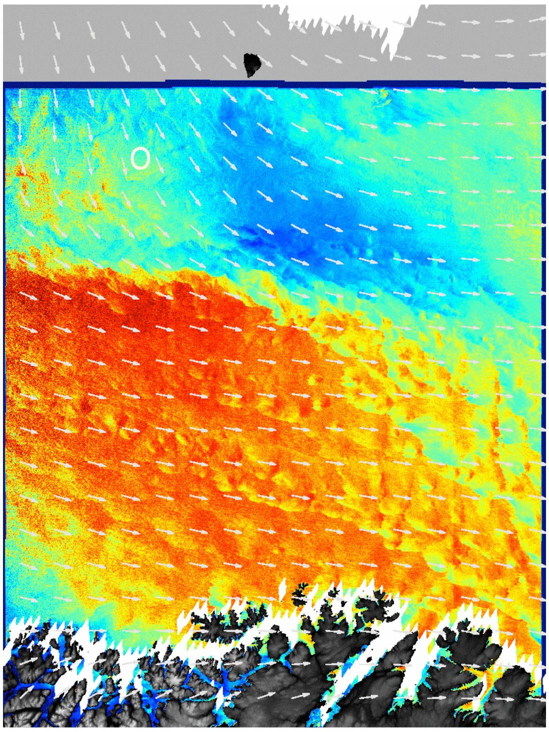

19 Mar 19:38

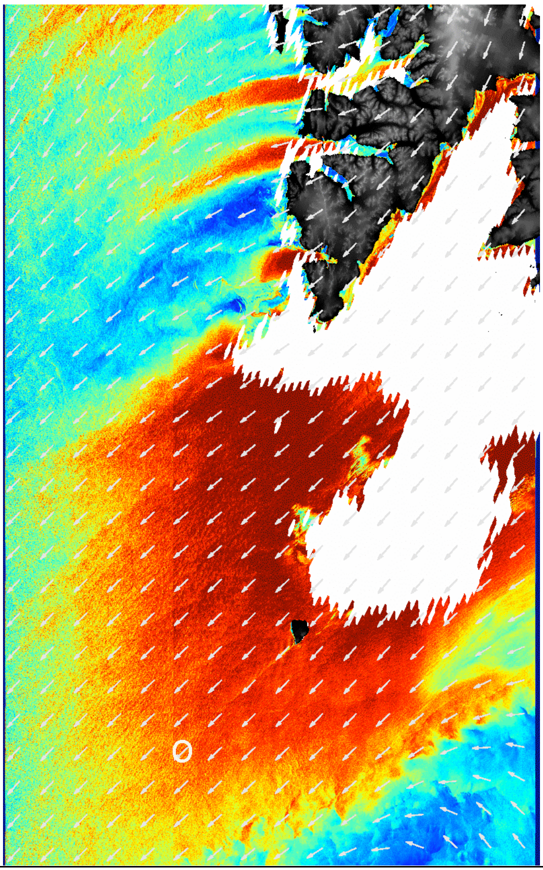

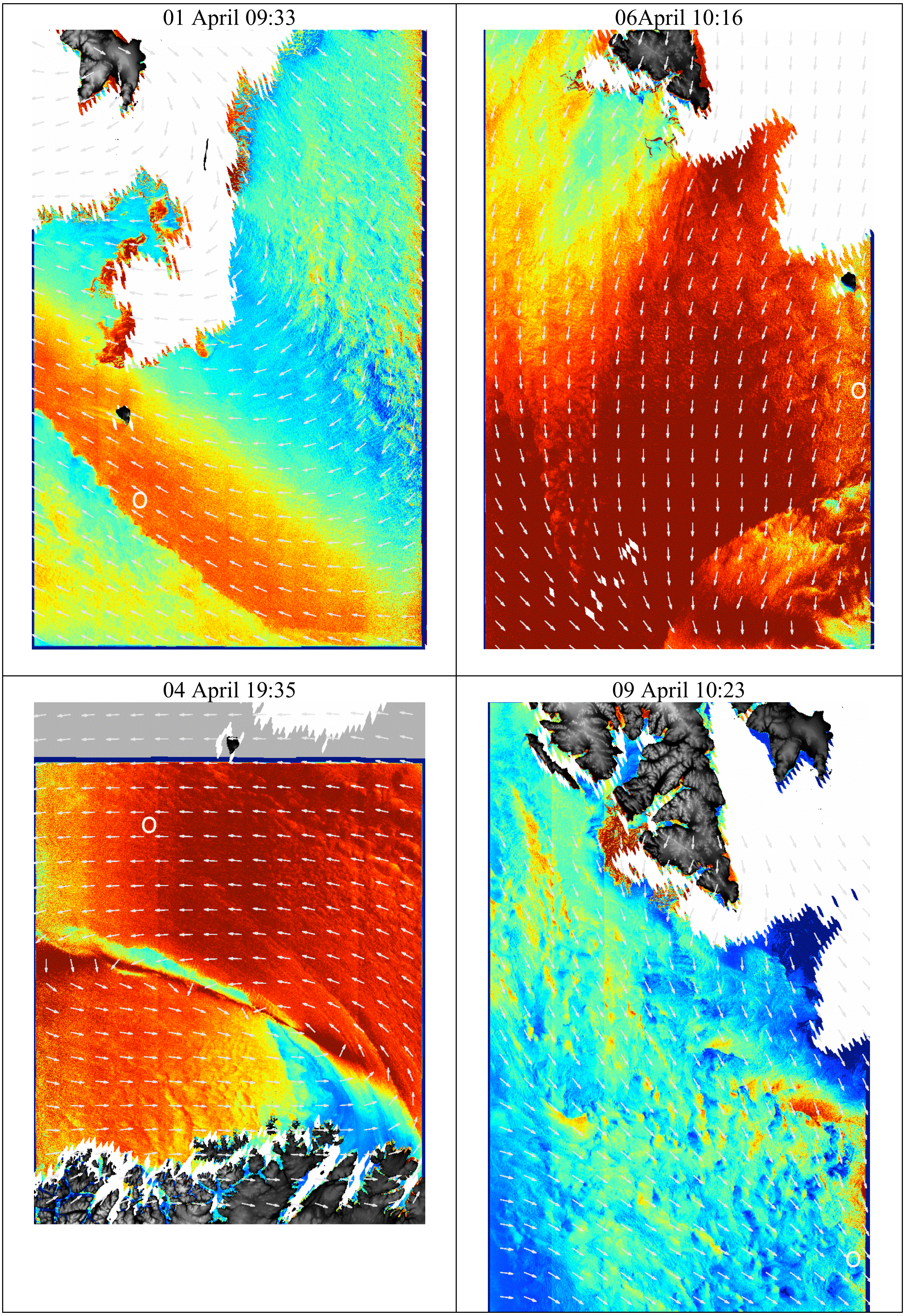
01 April 09:33
06April 10:16
04 April 19:35
09 April 10:23

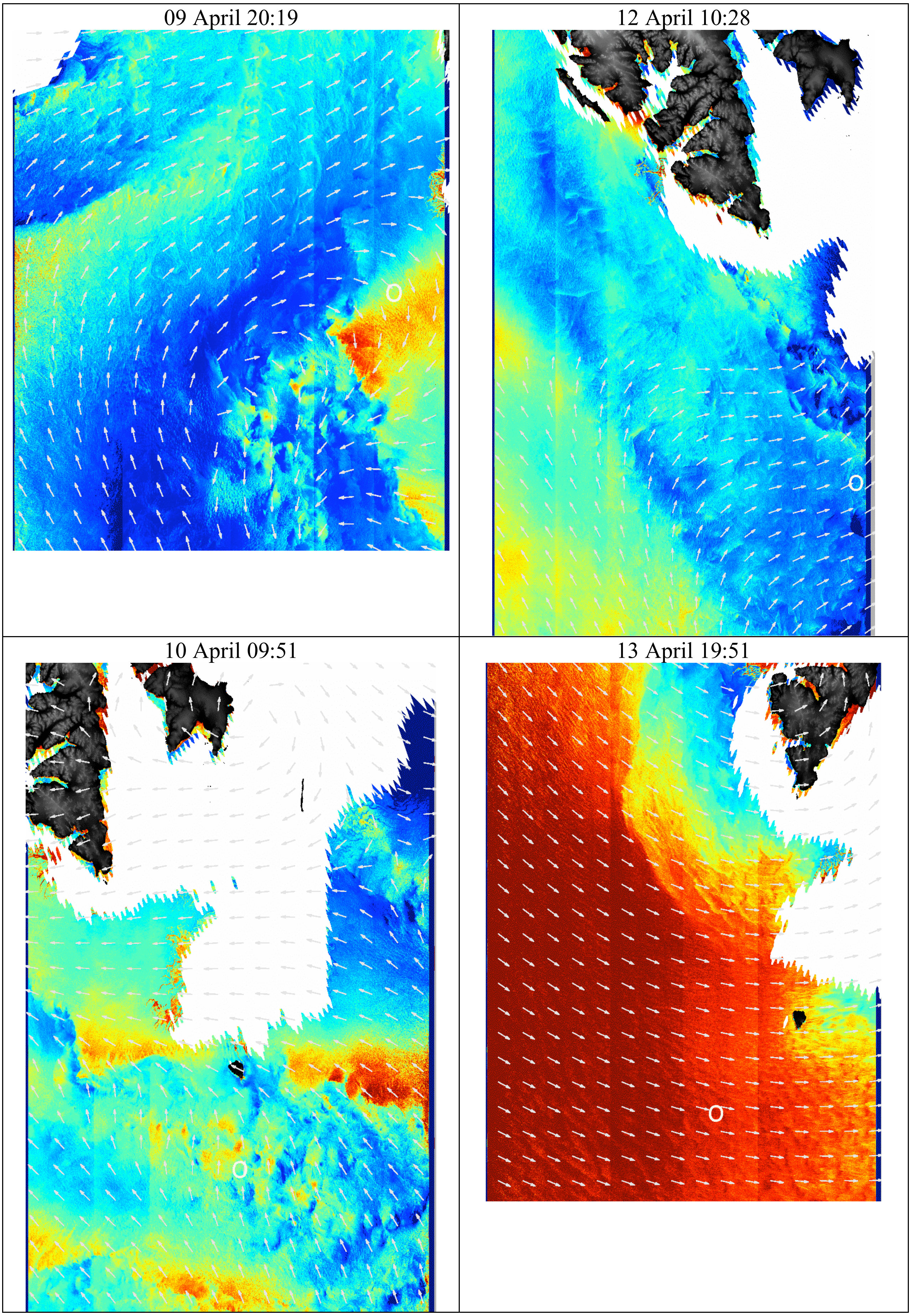
09 April 20:19
12 April 10:28
10 April 09:51
13 April 19:51

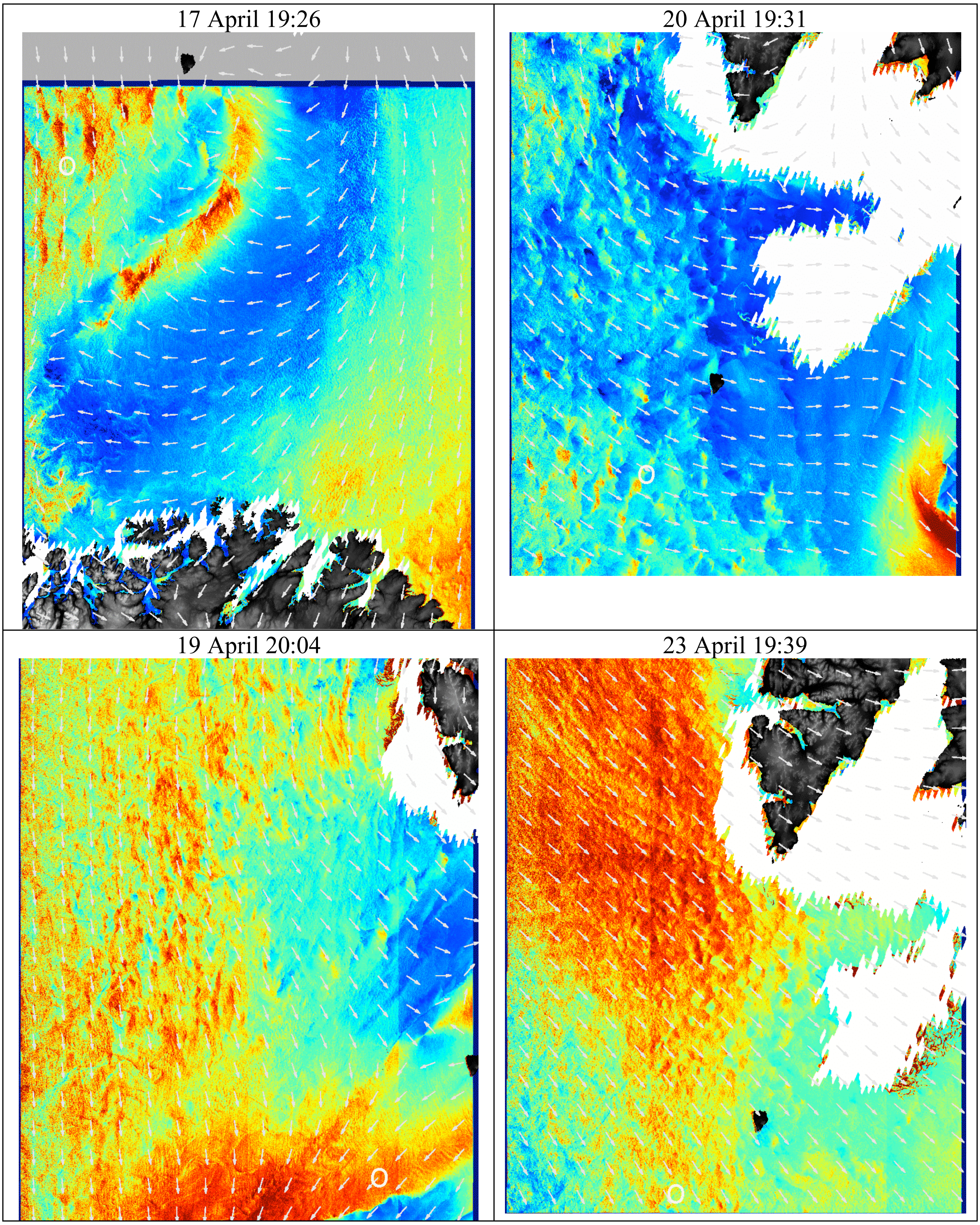
17 April 19:26
20 April 19:31
19 April 20:04
23 April 19:39

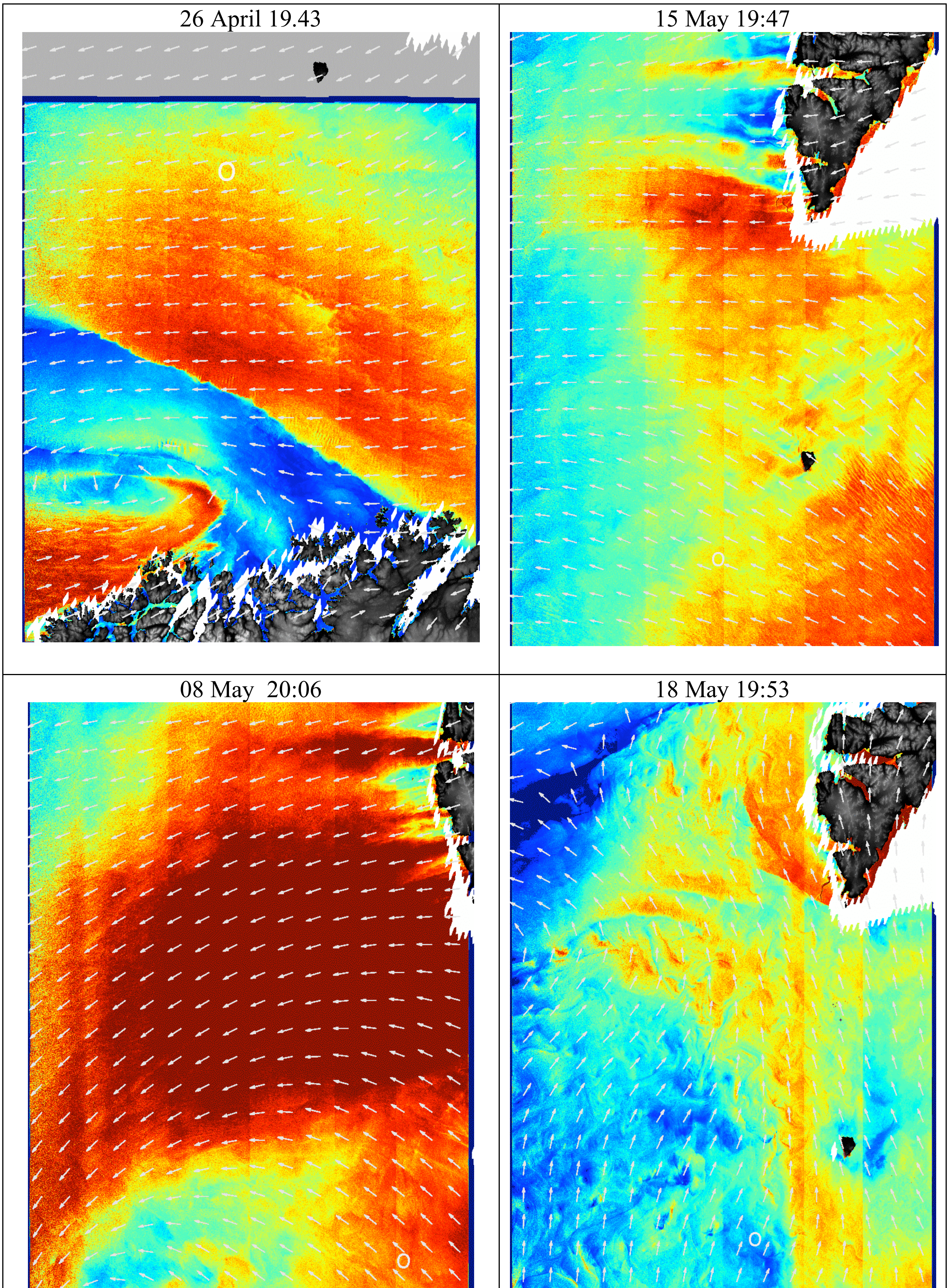
26 April 19.43
15 May 19:47
08 May 20:06
18 May 19:53

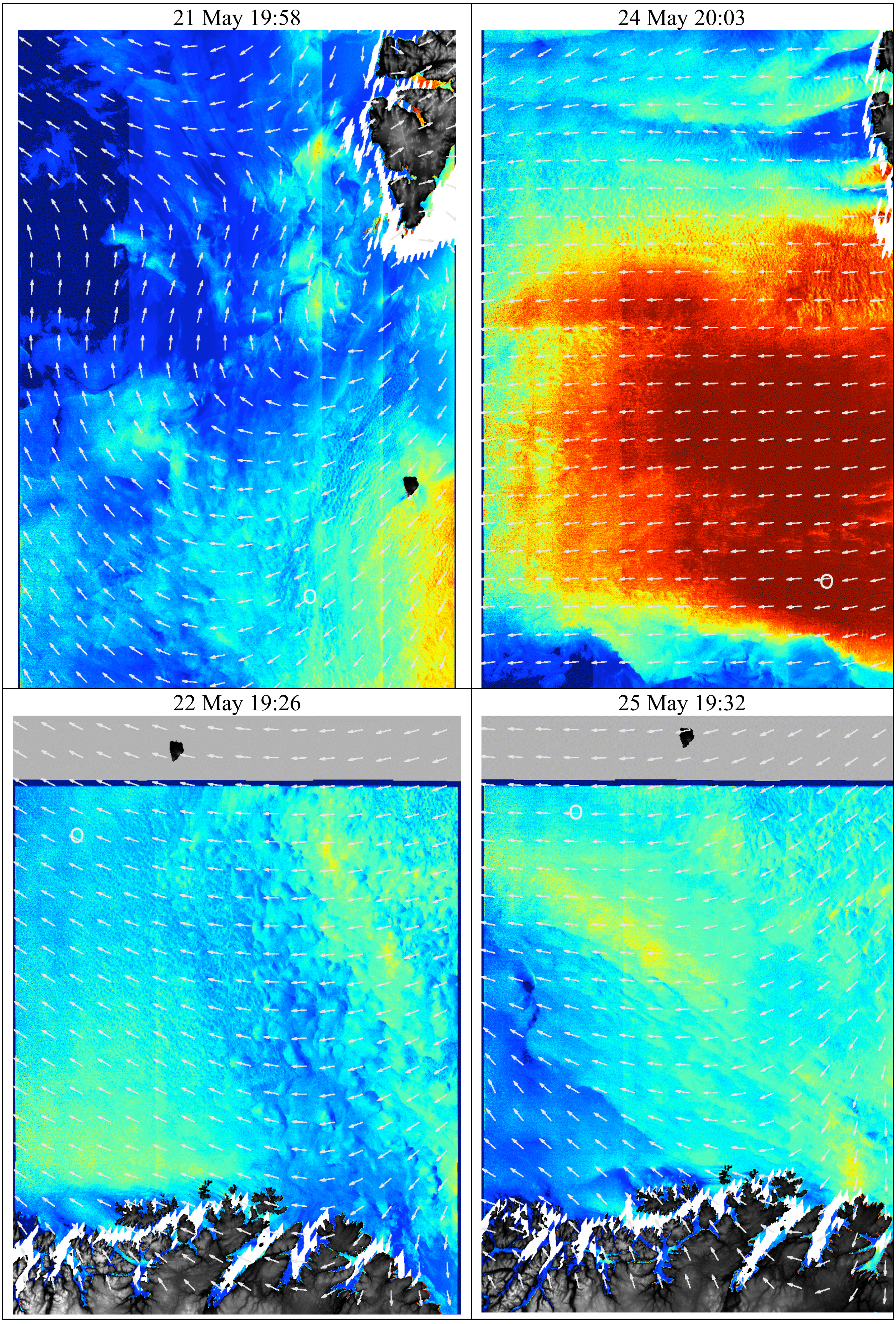
21 May 19:58
24 May 20:03
22 May 19:26
25 May 19:32

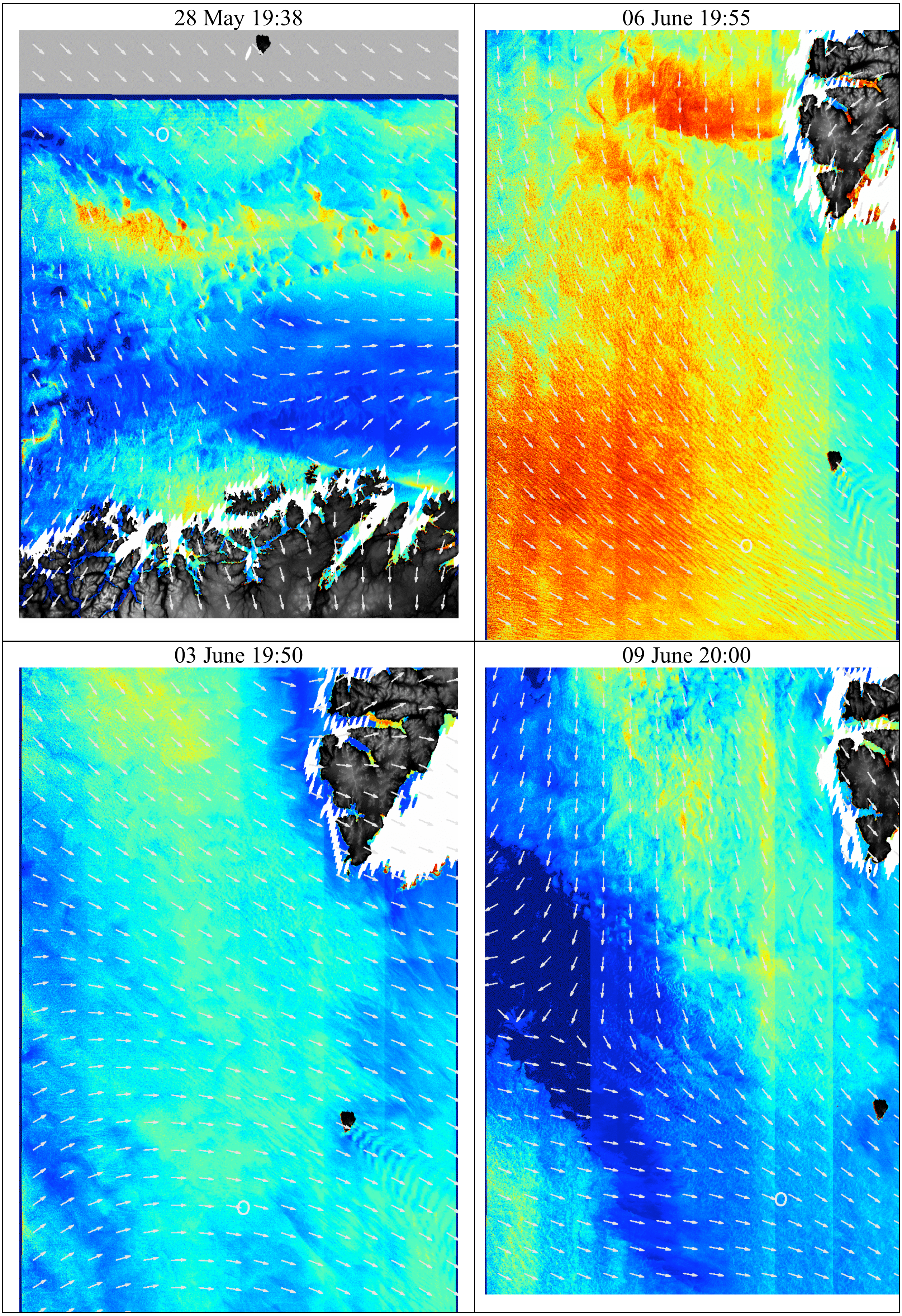
28 May 19:38
06 June 19:55
03 June 19:50
09 June 20:00

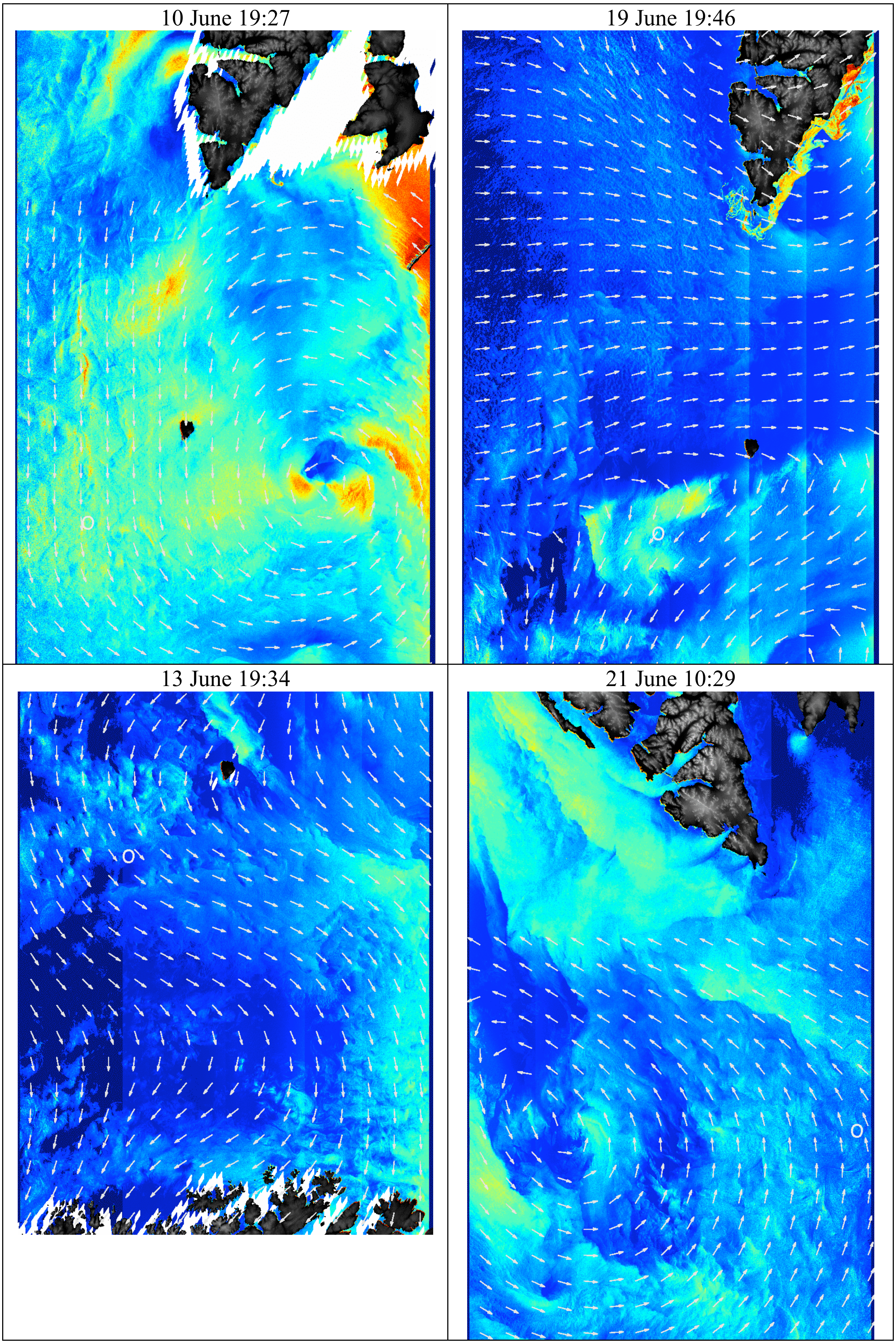
10 June 19:27
19 June 19:46
13 June 19:34
21 June 10:29

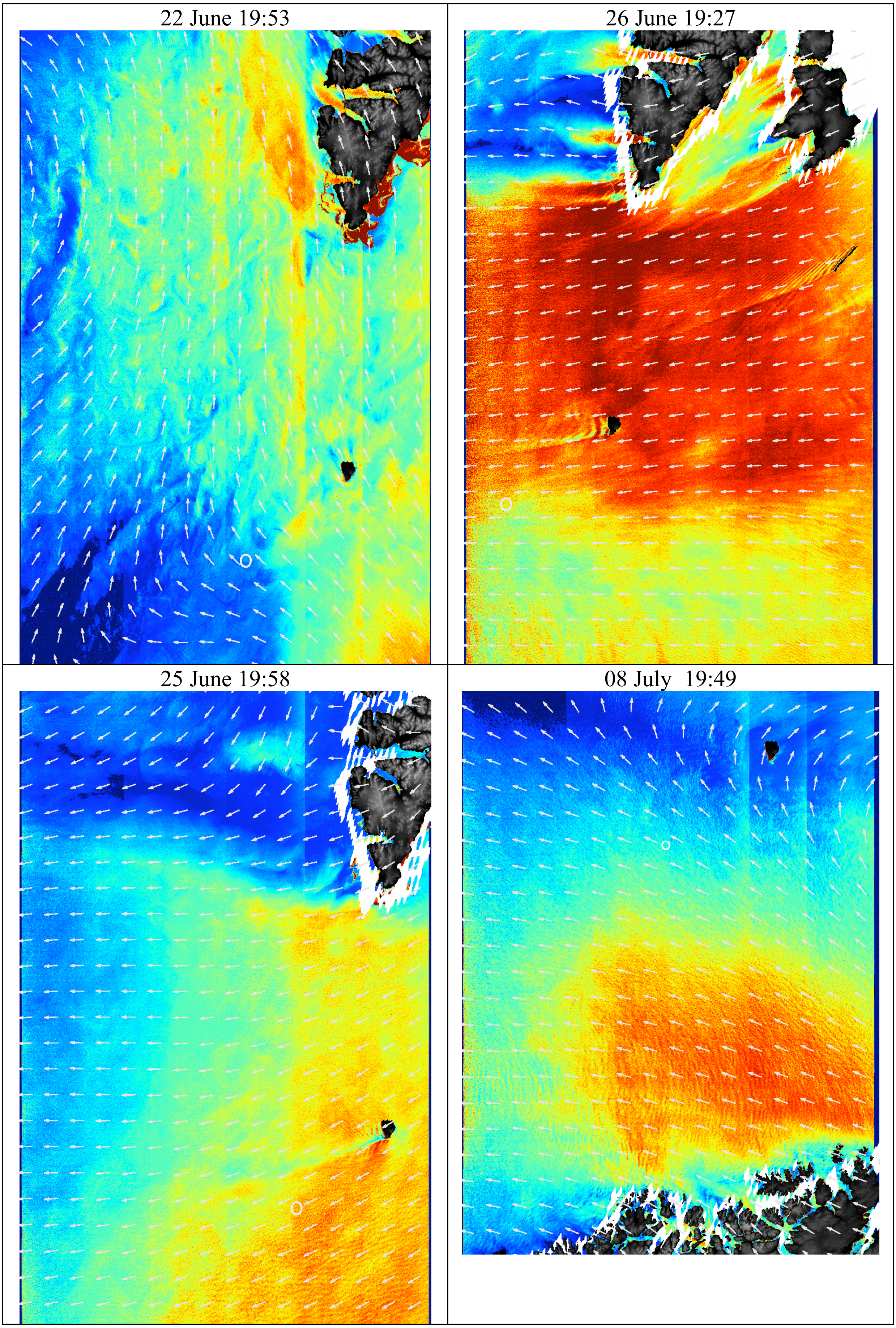
22 June 19:53
26 June 19:27
25 June 19:58
08 July 19:49

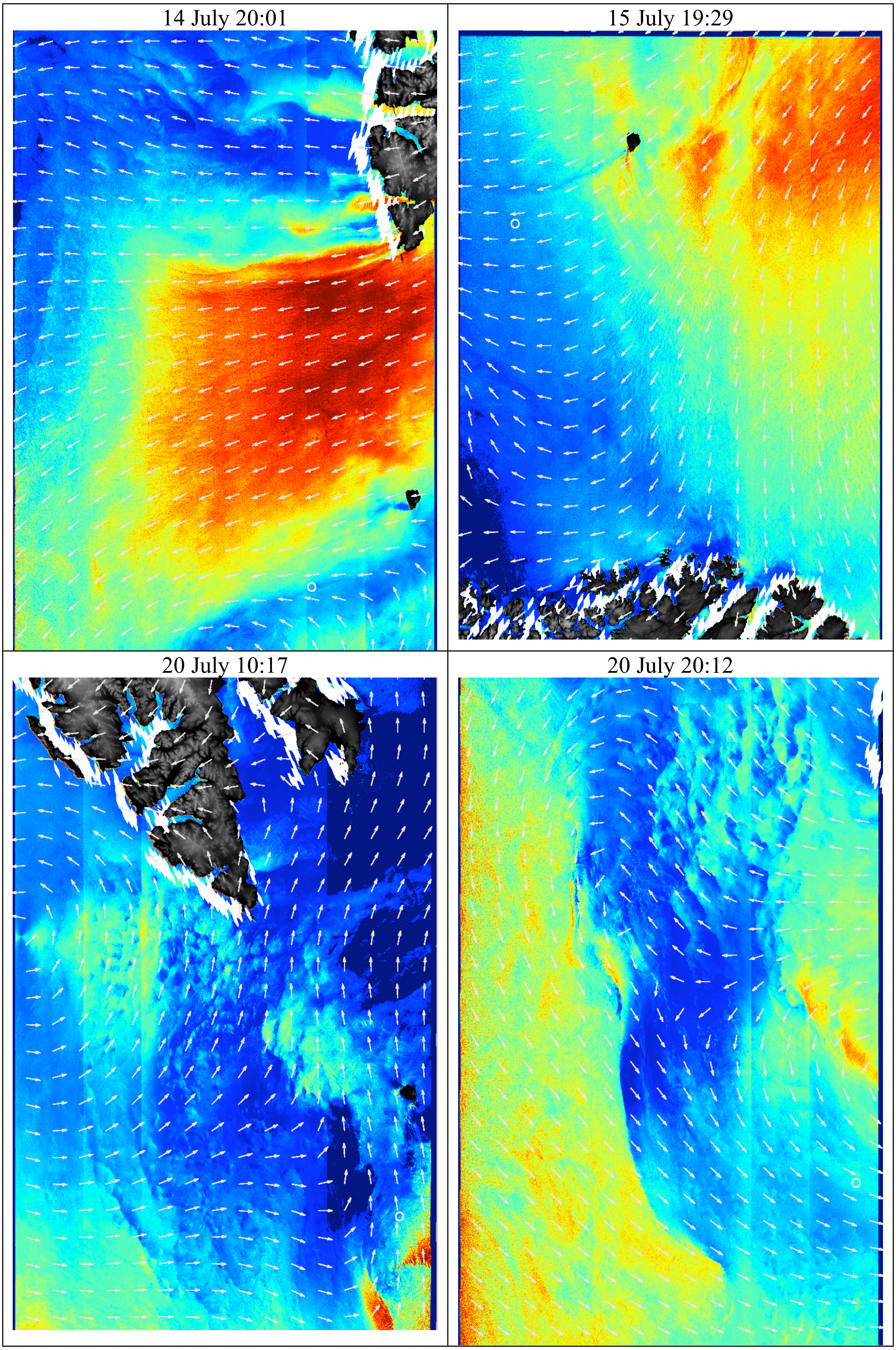
14 July 20:01
15 July 19:29
20 July 10:17
20 July 20:12

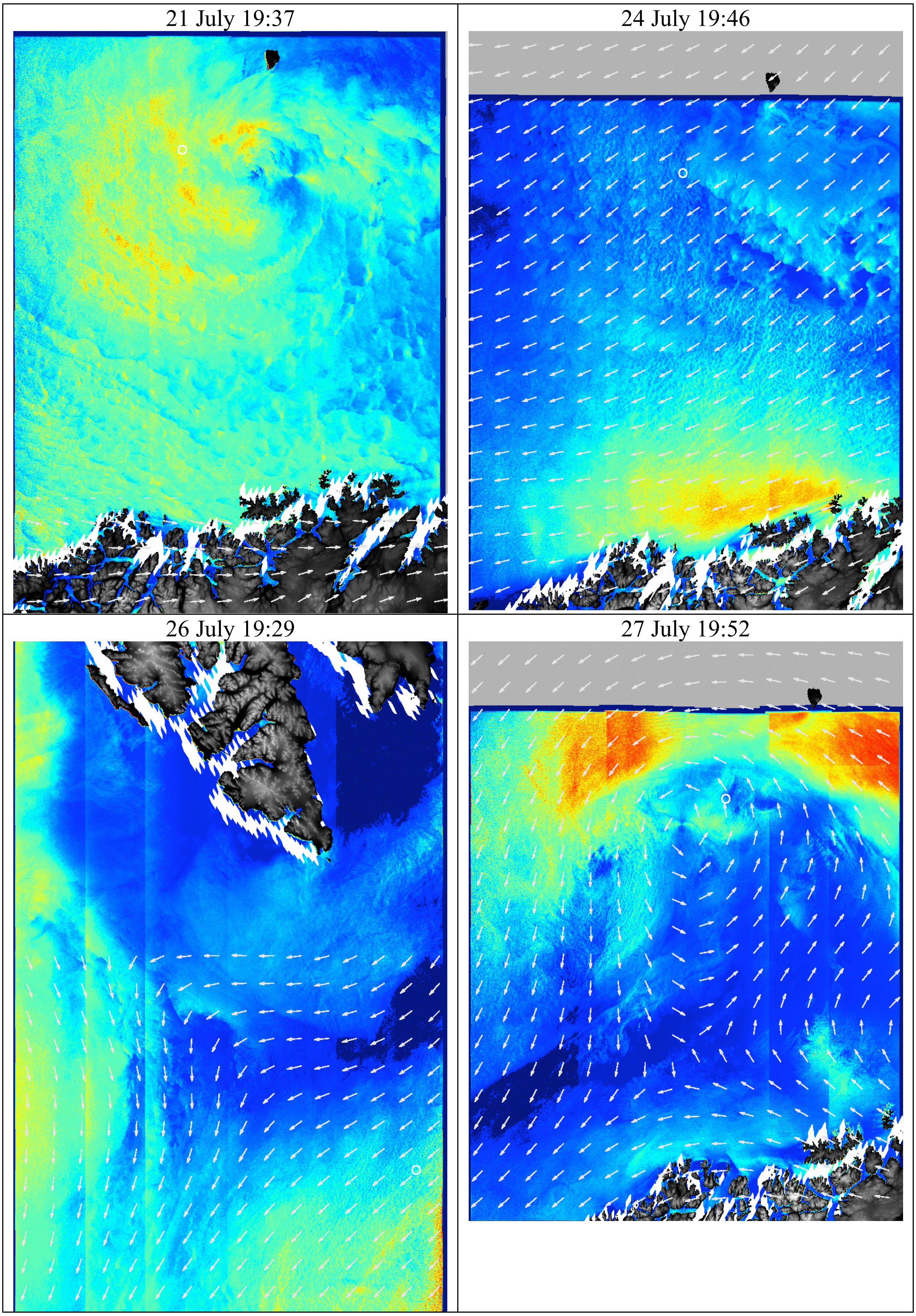
21 July 19:37
24 July 19:46
26 July 19:29
27 July 19:52

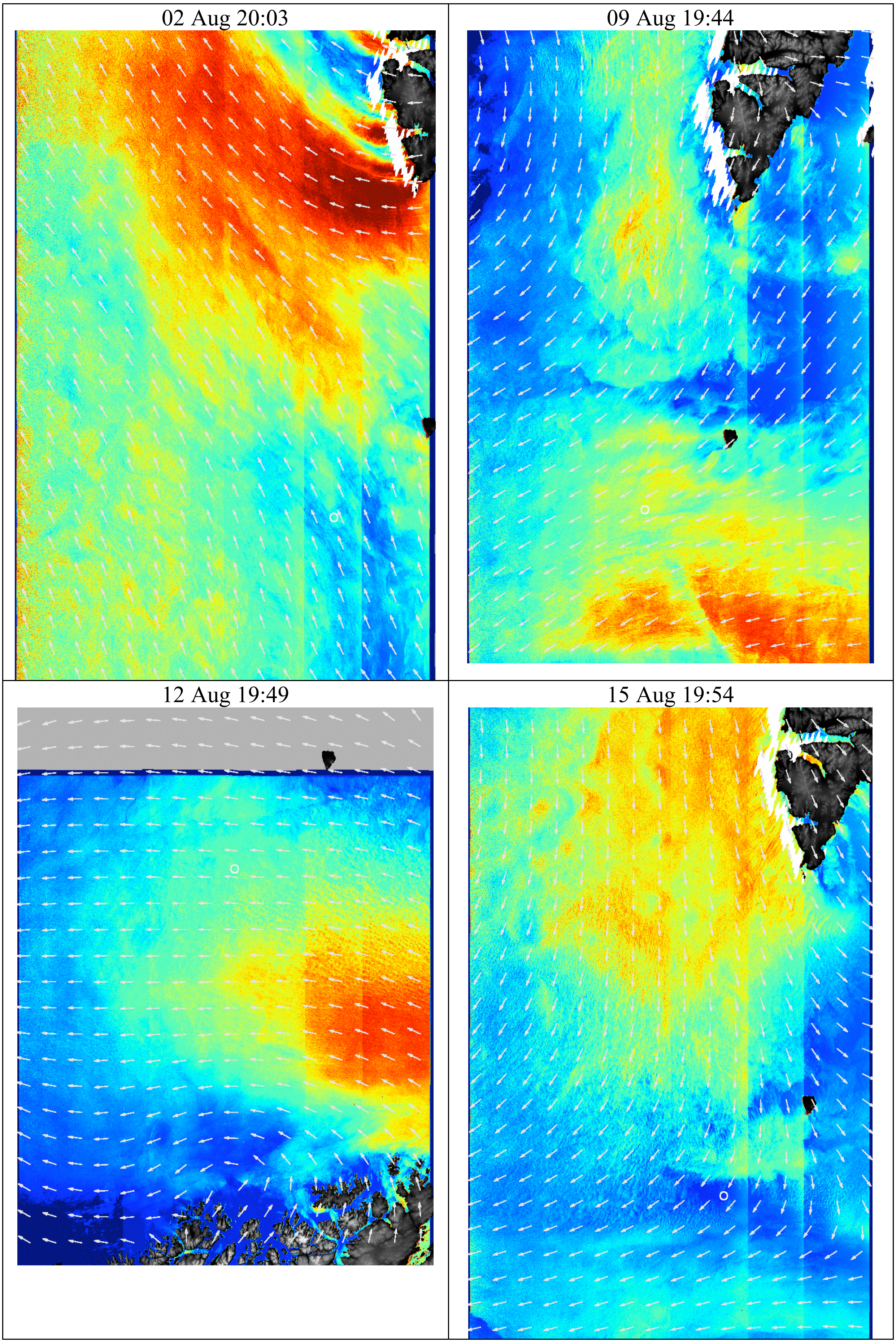
02 Aug 20:03
09 Aug 19:44
12 Aug 19:49
15 Aug 19:54

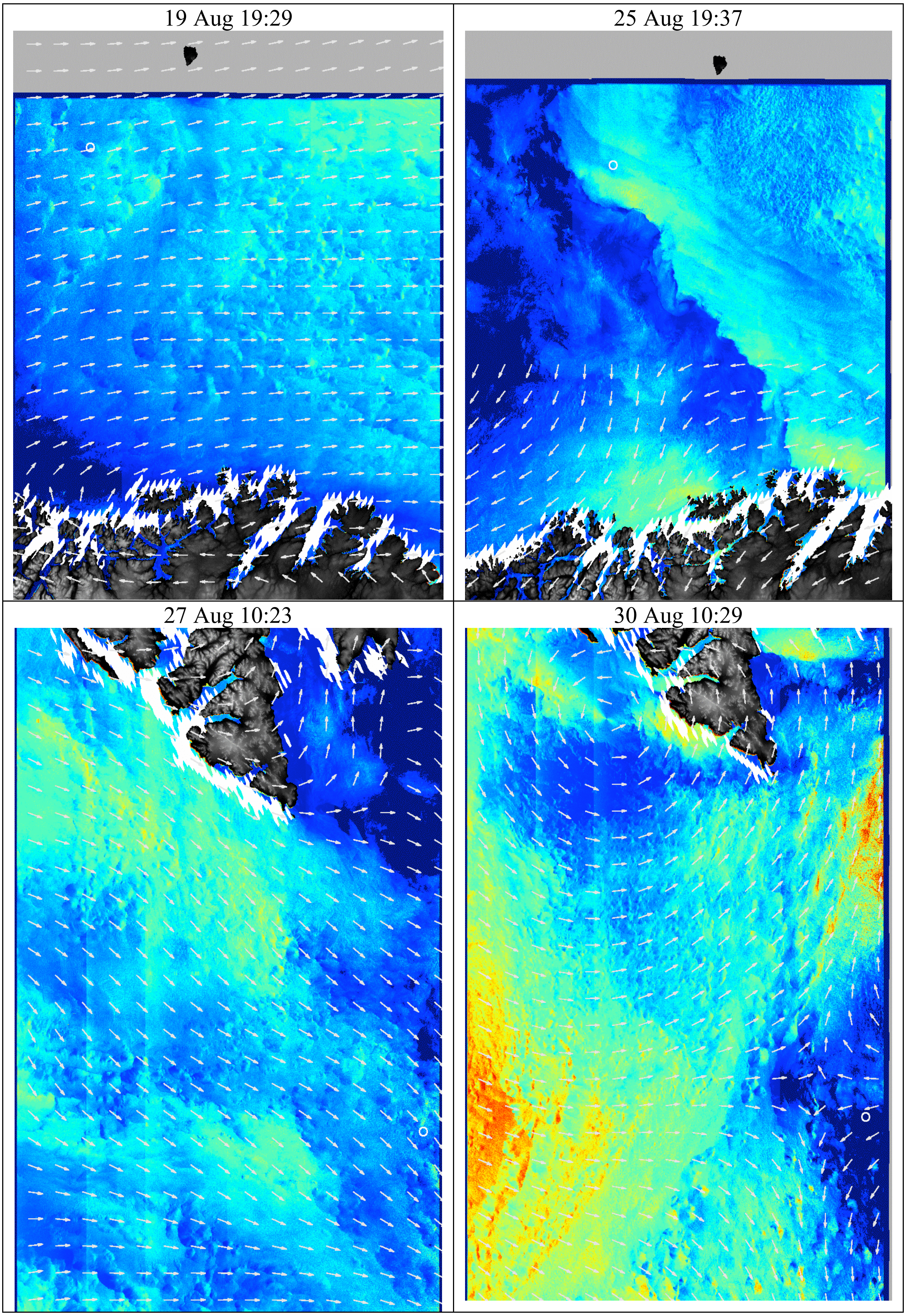
19 Aug 19:29
25 Aug 19:37
27 Aug 10:23
30 Aug 10:29

04 Sept 19:26

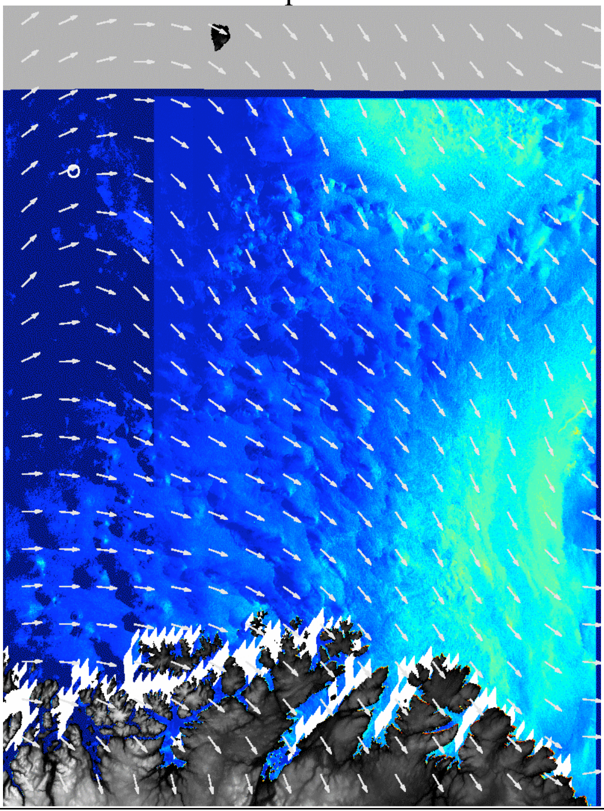

10 Sept 19:38

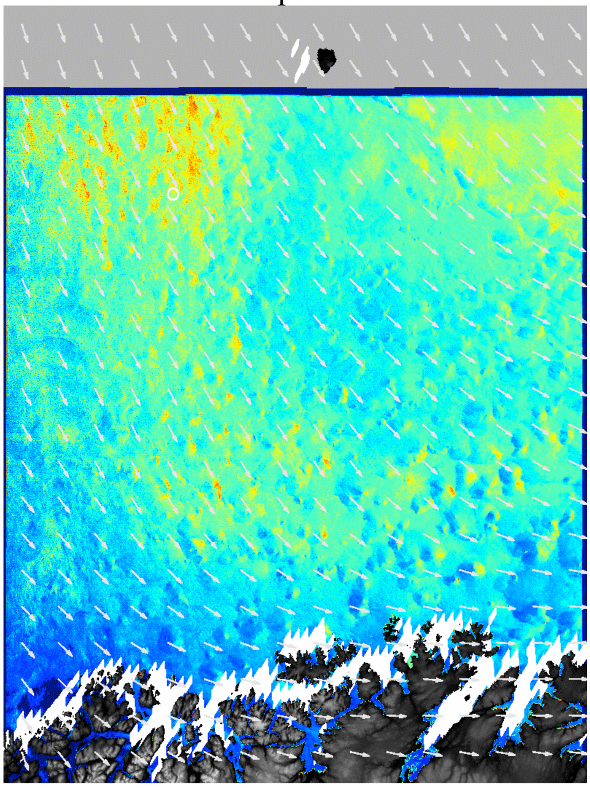

15 Sept 10:26

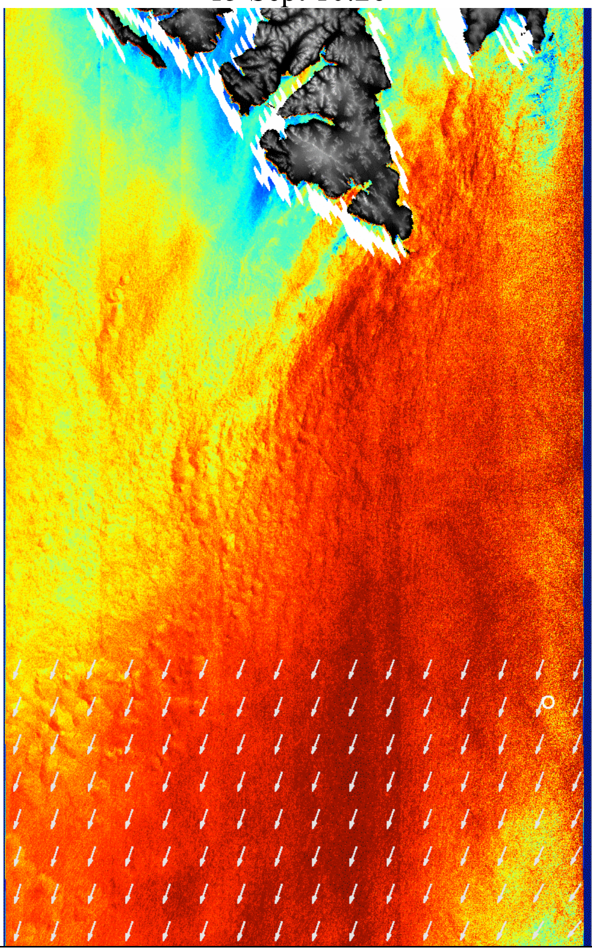

15 Sept. 20:20